Biomechanics of Infarcted Left Ventricle-A Review of Experiments

Wenguang Li

School of Engineering, University of Glasgow, Glasgow, G12 8QQ, UK

Date: 11/12/2019

Abstract

Myocardial infarction (MI) is one of leading diseases to contribute to annual death rate of 5% in the world. In the past decades, significant work has been devoted to this subject. Biomechanics of infarcted left ventricle (LV) is associated with MI diagnosis, understanding of remodelling, MI micro-structure and biomechanical property characterizations as well as MI therapy design and optimization, but the subject has not been reviewed presently. In the article, biomechanics of infarcted LV was reviewed in terms of experiments achieved in the subject so far. The concerned content includes experimental remodelling, kinematics and kinetics of infarcted LVs. A few important issues were discussed and several essential topics that need to be investigated further were summarized. Microstructure of MI tissue should be observed even carefully and compared between different methods for producing MI scar in the same animal model, and eventually correlated to passive biomechanical property by establishing innovative constitutive laws. More uniaxial or biaxial tensile tests are desirable on MI, border and remote tissues, and viscoelastic property identification should be performed in various time scales. Active contraction experiments on LV wall with MI should be conducted to clarify impaired LV pumping function and supply necessary data to the function modelling. Pressure-volume curves of LV with MI during diastole and systole for the human are also desirable to propose and validate constitutive laws for LV walls with MI.

Keywords: left ventricle; myocardial infarction; biomechanics; constitutive law, myocardium; viscoelasticity

Nomenclature

a	pressure-volume or tension-length model constant
b	pressure-volume or tension-length model constant
c	stress-strain or strain energy density function model constant
$\mathbf{C}$	right Cauchy-Green deformation tensor, $\mathbf{C} = \mathbf{F}^{\mathrm{T}}\mathbf{F}$
E_{es}	slope of the end systolic *p*-*V* relation
$\mathbf{F}$	deformation gradient tensor
$\mathbf{F}^{\mathrm{T}}$	the transpose of $\mathbf{F}$.
I_1	first invariant of $\mathbf{C}$, $I_1 = \mathrm{tr}(\mathbf{C})$
k_1	series elastic constant
k_2	stress-strain model constant
L	instantaneous segment length of left ventricle
p	left ventricular chamber/blood pressure
V	left ventricular chamber volume
p_{iso}	LV pressure during isovolumetric contraction
V_0	volume intercept of the end systolic *p*-*V* relation
V_{ce}	velocity of shortening of cardiac muscle
T	tension in left ventricle wall
α	property constant of static stress-strain curve
β	Stiffness of static stress-strain curve
ε	Lagrange strain or circumferential natural/logarithmic strain
$\dot{\varepsilon}$	strain rate
ΔLVEDV	% change in LVEDV
ΔLVESV	% change in LVESV
ΔSL	phasic segment-length amplitude
η	parallel viscous property constant
σ	Cauchy stress or circumferential stress
ψ	strain energy density function

Subscripts

0	segment length of left ventricle at end diastole before myocardial infarction
c	circumferential direction
l	longitudinal direction

Abbreviations

2CH	two-chamber
2D	two-dimensional

82	3D	three-dimensional
83	4CH	four-chamber
84	ACE	angiotensin-converting enzyme
85	ACI	apical conicity index
86	ACR	conicity ratio
87	ACS	abnormally contracting segments
88	BZ	border zone
89	CMR	cardiovascular magnetic resonance
90	CK-MB	creatine kinase myocardial band
91	CPK	creatine phosphokinase
92	CT	computerized tomography
93	CTR	cardiothoracic ratio
94	CV	cardiac volume
95	d	day
96	DTMRI	diffusion tensor magnetic resonance imaging
97	ED	end-diastolic
98	ECM	extracellular collagen matrix
99	EDL	end-diastolic segment length
100	DTPA	diethylenetriamine pentaacetic acid
101	EF	ejection fraction
102	ES	end-systolic
103	ESP	end-systolic pressure
104	ESV	end-systolic volume
105	ESVI	end-systolic volume index
106	h	hour
107	ICM	ischemic cardiomyopathy
108	LAD	left anterior descending
109	LCX	left circumflex
110	LCA	left coronary artery
111	LHD	left heart dimension
112	LGE	late gadolinium enhancement
113	LV	left ventricle
114	LVEDP	left ventricular end-diastolic pressure
115	LVEDV	left ventricular end-diastolic volume
116	LVEF	left ventricular ejection fraction
117	LVESV	left ventricular end-systolic volume
118	LVESP	left ventricular end-systolic pressure

MDCT multi-detector computed tomographic
MI myocardial infarction
MRI magnetic resonance imaging
mth month
MVO microvascular obstruction
NHS National Health Service
NICM non-ischemic cardiomyopathy
PCA principal component analysis
RCA right coronary artery
SEM standard error of the mean
SI sphericity index
SPECT single-photon emission computed tomography
STEMI ST-elevation myocardial infarction
SV stroke volume
SW stroke work
VP visceral pericardium
WHO World Health Organization
wk week
y year

1 Introduction

Myocardial infarction (MI) indicates death of the cells of an area of the myocardium due to the lack of oxygen caused by obstruction of the blood supply, see Fig. 1. The myocardium has its blood supply from the two large coronary arteries such as left circumflex (LCX) and left anterior descending (LAD) arteries and their branches. Occlusion of one or more of these vessels is the major cause of MI. Based on a WHO statement, there are 17.4 million MIs worldwide every year in comparison with 15 million strokes. Survivors of MI have annual death rate of 5%, which are six times that in peoples of the same age who do not have coronary heart disease [1]. In the UK prevalence of coronary heart disease is 4.5% in the North East of England, and 4.3% in Scotland. The NHS in England spent around £6.8 billion on the disease in 2012-2013 [2].

After acute MI, the left ventricle (LV) will undergo a healing processing, which includes acute ischemia (the first minutes to hours after MI), necrotic/dying phase (the first a few days), fibrotic phase (weeks and months after MI) and remodelling phase (months after MI), which is regulated by mechanical, neuro-hormonal and genetic factors [3]. During the process, the LV can be subjected to dilation, thinning of infarct zone, hypertrophy and fibrosis (collagen fibre scar) sequentially and can be in risk of heart failure or rupture [4], which remains a major source of morbidity and mortality [5]. This progressive remodelling process is an important determinant of the clinical course of heart failure [6].

There have been a significant number of comprehensive and elegant reviews of acute MI, such as those [5] for MI various clinical features, [6, 9-15] for remodelling mechanisms, pathology and therapy, [16] for mechanisms of adverse remodelling (LV enlargement and dilation) and reverse remodelling (LV shrinkage) and prevention of adverse remodelling after MI, [17] for structural and mechanics of healing MI, [18-22] for MI therapy, [23] for MI diagnosis and treatment, [24] for acute MI earliest diagnosis, [25-29] for MI imaging, [30, 31] for heart failure due to MI, [32-34] for LV rupture and [35] for biomaterial strategies to alleviate MI, [36] for cellular, molecular mechanisms and therapeutic modalities after MI, and [37] for microvascular obstruction (MVO) post-MI to name a few so far. Their contents are no longer repeated hereby.

Biomechanics of infarcted LVs is the study of the structure, function, kinematics and kinetics of infarcted LVs at organ, tissue and cell levels by employing experimental and mathematical modelling methods of mechanics. It has experienced a rapid and significant development since 1960's and has played a vital role in MI diagnosis, understanding of remodelling, MI micro-structure and biomechanical property characterizations as well as MI therapy design and optimization.

The changes in LV wall passive properties and myocardium structure were reviewed in terms of acute ischemia, necrotic, fibrotic and remodelling phases thoroughly in [17] with emphasis on MI scar healing, and a benchmark has been established in the field. In this contribution, the literature of experimental studies on infarcted LVs was sorted out in biomechanics context, i.e. kinematics and

kinetics of LV with MI at organ, tissue and microstructure levels, especially fresh literature that was published in more than 10 years after [17] was reviewed. The aim of the paper is to provide a supplement for existing review papers on the subject and help researchers develop new ideas as well as offer some evidence to biomechanics modelling of infarcted LVs.

The paper covers experimental remodelling, kinematics and kinetics of LV with MI. The experimental remodelling is the basis for the understanding of the others; hence it is explained at first from the biomechanics worker's point of view briefly. If one has been familiar with it, this part can be ignored. The experimental outcomes of LVs with MI seem to be reviewed in terms of kinematics and kinetics of biomechanics for the first time, naturally such a summary might be helpful for further investigations in these two subjects.

Note that experimental studies on LVs with MI are mainly related to animal models. Here some clinical investigations based on the human, which have direct contributions to kinematics and kinetics of biomechanics of infarcted LVs, were carefully selected and included.

2 Experimental remodelling

2.1 MI histology

MI histology includes MI size, location and morphology. The morphology mainly refers to collagen fibre microstructure in MI scar. Microscopic observation and modelling of collagen fibre growth in MI scar have increasingly become an interesting research issue. Late gadolinium enhanced (LEG) MRI is the most precise in vivo technique for determining MI size and location in LVs. MI can appear in anterior, lateral, posterior and septal positions of LVs, but commonly in anterior location. A larger anterior MI can lead to significant LV dilation. MI size can impair LV pumping function, even results in heart failure; especially, the size is negatively and linearly correlated with follow-up LVEF. The myocytes in MI zone disappear and collagen fibres will grow post-MI, the collagen fibre structure is with more organization, i.e. oriented circumferentially in MI zone near LV equator than at the apex. When acute MI occurs, the LVs need to be reperfused as soon as possible. In the MI zone, there are some isolated areas that the reperfusion is invalid, called microvascular obstruction (MVO). MVO can induce more cardiovascular complications and prompt adverse remodelling and delay LV function recovery.

2.1.1 MI size and location

There are four methods for measuring MI size in a LV. The first method is radioautographic method in which radioisotope-labelled microspheres in 7-10 or 20μ are injected into blood and their concentration in LV tissue is extracted from radioautograms of harvested LV tissue samples after MI and the volume with low microsphere concentration is the MI region [38].

The second method is based on the changes in cardiac marker, such as creatine phosphokinase (CPK) or creatine kinase myocardial band (CK-MB) [39] or troponin [40] in blood after MI. CPK is an enzyme in myocardial cells that is sensitive and relatively specific indicator of the extent of ischemic injury following acute coronary occlusion [39]. Based on this fact, MI size was estimated mathematically based on analysis of serial serum CPK changes [41].

The third method is technetium-99m sestamibi single-photon emission computed tomography (SPECT) myocardial perfusion imaging [42], and the last method is MRI-based, late contrast agent-enhanced in vivo approach. The methods for measuring infarct size have been reviewed throughout in [43].

Gadophrin-2 is a new MRI contrast agent with high affinity for necrotic myocardium, and an in vivo gadophrin-2-ehnanced MRI can determine infarct size precisely based on a canine model [44]. Then a gadolinium-based contrast agent with high spatial resolution was found and used to enhance MRI for accurately identifying infarct size of acute MI [45]. This in vivo technique was employed to identify reversible myocardial dysfunction post-MI in [46]. Currently, this method has been intensively applied in infarct size estimation [47-49]. Numerous automatic algorithms for quantifying MI size accurately have been developed in [50-63]. Methods for assessment of acute MI have been recommended in [64].

Based on the rat model, for small MI size (4-30)%, which is the ratio of the MI surface area over the LV surface area, there is no discernible impairment in haemodynamics, LV pumping function and pressure generated in comparison with those of the control subjects. Rats with moderate (31-46%) infarct size, have normal haemodynamics, but reduced peak blood flow and developed pressure. Rats with infarct size more than 46% have a congestive heart failure [65].

For rupture LVs, infarct zone is located at anterior (42%), lateral (21%) and posterior (37%) position of LV, respectively; for no rupture LVs, however, the zone is in anterior (66%), lateral (10%) and posterior (24%) [66], suggesting the anterior side at great risk of MI occurrence. The other survey demonstrates that infarct zone is onset in anterior (52.8%) and posterior (inferior) (47.2%) almost equally [67]. In 61 MI patients, 52.5% of them suffered from anterior MI and 47.5% from posterior MI, the patients with large anterior MI had the worst dilation course [68].

Many clinical trials, such as those in [69-77] to name a few, have exhibited that initial infarct size is a stronger and independent index to predict remodelling and mortality in patients with MI at 6mth or 1y after MI than left ventricular ejection fraction (LVEF), end-systolic volume index (ESVI) and contractile reserve.

For 20 acute MI patients, their MI size is decreased linearly with increasing follow-up LVEF, exhibiting a good correlation; additionally, peak troponin rises with increasing MI size lineally [78]. Similar work illustrates that there is a negative linear relationship between infarct size in patients with infarct size $\geq$15% at 3mth after MI, otherwise no obvious relationship between two factors [79]. The relationship between infarct size and the incidence of cardiac arrhythmias during MI was examined

[80], it turns out that the arrhythmias is positively correlated with infarct size, but also subject to a remarkably increased 1y mortality. For diabetic patients with MI, their infarct size is modestly larger than non-diabetic patients, especially, the former is subject to a higher (4-6fold) mortality rate than the latter [81].

2.1.2 MI morphology and collagen fibre structure

After MI, the dead myocardial tissue will be replaced by newly grown collagen fibres gradually. MI morphology is mainly associated with microstructure of these collagen fibres. In experiments made in [82], at 24h after MI in the rat LVs, there is significant collagen degradation in the infarcted zone medicated by inflammatory cell proteases.

Infarct zones become the scars after MI, which mainly consist of collagen fibres of type I. Collagen orientation of dog LV was measured by using polarized light microscopy, and it was shown that the molecular organization of scar collagen increased from 1 to 6wk after MI, particularly, sub-epicardial collagen fibres were obliquely alighted (-14.0 ± 3.5^{o}), mid-myocardial collagen fibres circumferentially alighted (-1.4 ± 0.4^{o}), while sub-endocardial collagen fibres obliquely alighted(-12.7 ± 2.1^{o}) [83].

In the rat LVs at 13wk after MI, collagen concentration and degree of covalent cross-linking of collagen fibrils increased in viable myocardium in comparison with the control, the scar exhibited further increase in both collagen concentration and degree of covalent cross-linking of collagen fibrils [84].

Based on the pig model, orientation of large collagen fibre in the scar was examined at 3wk after MI and the mean fibre angle was less than 30^{o} measured from the circumferential direction. This small fibre angle allows the scar to resist circumferential stretching while deforming normally compatibly with adjacent normal myocardium in the longitudinal and radial directions. The similar results in the pig LV model can be found in [85].

Three groups of infarcted pigs were employed, Group 1 was used as infarct controls, Group 2 had the endocardium slit longitudinally to alter local systolic deformation and Group 3 had a plug sectioned from MI tissue and rotated 90^{o}. The mean fibre angle cannot be altered by the endocardium slit and plug [86]. In the rat model, infarcts near the equator of the LV stretched basically in the circumferential direction and developed circumferentially orientated collagen, infarcts at the apex, however, stretched in the circumferential and longitudinal directions and developed randomly alighted collagen [87], as shown in Fig. 2.

The organization of collagen fibres was investigated in 100 swine and 95 human patient samples by reperfusion at 1wk (acute MI) and 1mth (chronic MI) after MI. there was no difference in collagen organization between the acute and chronic groups. Collagen fibres demonstrated an organized pattern in the core of the infarct scar, in the outer region, however, the fibres showed quite less organization, i.e. a significant inhomogeneity [88].

Cardiac fibre structure at 4wk after MI in the rats was measured by using diffusion tensor magnetic resonance imaging (DTMRI) technique in [89]. It was identified that transmural courses of myofibre orientation angles in MI zone were similar to those in remote healthy zone. The newly produced collagen fibres in MI zone might maintain the original orientation of the myofibres they replace.

Ultrasonic backscatter method was applied to measure the transmural shift in fibre orientation per millimetre in normal and MI cardiac tissues [90] and the shift in the MI areas is 59% bigger than that in the normal cardiac tissue (9.2±0.7°/mm).

A similar result was found out in the sheep model at 6wk after MI in [91]. Further, after left ventricular surgical restoration, aneurysm plication just allowed myofibres in the anterior border zone to rotate counter-clockwise (-35.6 ±10.5^{o}) and those in the lateral border zone to rotate clockwise (34.4±8.1^{o}), suggesting surgical restoration technique might fail to restore normal myofiber transmural orientation angle profiles.

For the rat and pig models, healing scars increase in collagen content with time, but still are structurally isotropic at 1, 2, 3 and 6wk after MI [92]. In the unloaded rat LVs with MI, collagen fibre deposition can increase significantly in the remote region and the collagen fibre orientation becomes more disorder in the MI zone compared with the LVs without unloaded condition [93].

2.1.3 Microvascular obstruction

MVO is known as the 'no-reflow' phenomenon in infarcted region due to injury to microvasculature, i.e. capillary, and subsequent obstruction by erythrocytes, neutrophils and debris caused from reperfusion after MI [94]. MVO was identified by using contrast-enhanced echocardiography and MRI successfully and it was found that the extent of MVO was unchanged at 2d and 9d after reperfusion based on the dog model [95]. The other study showed that the extent of MVO increased significantly over the first 48h after MI by employing gadolinium-DTPA-enhanced MRI [96]. Patients with MVO had more cardiovascular complications than those without MI at 10d after MI, in follow-up MRI (at 16mth post-MI), the patients with MI were related to fibrous scar formation and LV remodelling [97].

LGE and MRI 3D-tagging were conducted at 4h to 6h and 48h and 10d on the dogs after reperfusion post-MI and the circumferential, longitudinal and radial strains and the first principal strain were determined from images. Extent of MVO had better and independent value to predict LV volume than the total infarct size did. The first principal strain was strongly and inversely correlated with relative extent of MVO in infarcted tissue, and extent of MVO could reduce circumferential and longitudinal strains as well as radial thickening in infarcted zone [98].

The size and transmural extent of reperfused infarct in patients decreased from week 1 to week 8 after MI, especially for MIs with MVO, unfortunately, regional and global LV function for infarcts with MVO didn't improve more significantly than the function for infarcts without MVO did

[99]. A similar investigation demonstrated that presence of MVO was related to more extensive infarcts and resulted in more marked adverse remodelling and delayed LV function recovery [100].

Seventy-one patients with MI underwent cardiovascular magnetic resonance (CMR) imaging, myocardial tagging and LGE at 2-6d after reperfusion, regional circumferential and radial strains and corresponding strain rates, absolute and relative wall thickening were determined in 16 segments. Strains could discriminate more precisely between non-infarcted myocardium and infarcted myocardium with and without MVO than wall thickening index. Peak circumferential strain was the most accurate index of regional LV function in comparison with absolute and relative wall thickening [101].

2.2 Observed remodelling process

Remodelling process is the recovery process of partial loss of LV normal pumping function from around the 2^{nd}-5^{th} day post-MI. In the process, infarct zone undergoes expansion and extension. Expansion means regional dilation and thinning of the area of infarction, but extension indicates the occurrence of additional myocardial necrosis caused from reperfusion. The infarcted zone is shrunk along with compensatory expansion of remote zone, and collagen fibres start to deposit to form a scar up to 6wk. A remodelling process is favourable to lowering LV diastolic pressure and increasing cardiac blood output, but a sustained LV dilation can lead to LV dysfunction. If LV function is recovery in terms of stroke volume and ejection fraction (EF) after a remodelling process, then this remodelling process is called reverse remodelling, otherwise adverse remodelling.

Clinical studies showed severe expansion did not develop until 5d after MI (59% of 76 patients) [102]. Twenty-one transmural and 18 non-transmural infarcts of 1-11d of ages in the dog model were created, and their expansion was observed in terms of survival day. For infarcts, the survival day was correlated negatively and linearly with a variable expressed by infarct size (the ratio of the infarct weight to the LV weight) and extent of expansion (the ratio of the infarct circumferential length to the non-infarct circumferential length) [103].

In 84 rats, infarcts were developed by ligation of the left coronary artery (LCA) and investigated at 1, 2, 4, 5 and 7d. Expansion was observed in 61% of transmural infarcts at 1-2d, in 65% at 3-4d and 80% at 5-7d. The percentage of rates with severe expansion rose from 0% at 1-2d, to 23% at 3-4d to 65% at 5-7d. This infarct evolution was roughly two-fold of that of human and the critical infarct size for severe expansion is at least 17% [104].

Infarcts in 22 rats were produced and their lengths, circumferences and areas of the LV, of the infarcted myocardium and of the non-infarcted myocardium were observed at 2 and 21d. It was shown that early changes (in 2d) in structure post-MI included LV tissue loss accompanying with LV chamber dilation, and later changes (in 2-21d) were composed of shrinkage of infarcted tissue along with compensatory expansion of non-infarcted tissue [105].

Temporal changes in infarct collagen and LV topography during healing after MI were measured with 132 dogs under coronary artery ligation condition at 1, 2, 7d, 2, 4 and 6wk. In the first 7d, LV cavity dilation and infarct expansion emerged, and then infarct contraction and thinning as well as collagen deposition were followed up to 6wk. Thinned infarcted segment and collagen deposition are responsible for LV regional shape distortion post-MI [106].

Dogs were anesthetized, marker positions in their LVs were recorded and 3D coordinates were reconstructed before and 1, 24h and 1wk after infarction. At 1h after MI, ED areas in infarct area increased by 20.3% above the control compared with 7.9% in the remote region; at 24h post-MI, both the regions expanded by additional 10.0%; at 1wk, the infarct ED area was 31.4% above the control, but the remote area decreased to 8.5%. Thus, infarct dilation emerges in 1h post-MI along with remote dilation as a compensatory response. Even though the infarct area is maintained to dilate sustainably, the non-infarct region compensatory dilation becomes less by 1wk [107].

LV volume index and haemodynamic pressure of 29 MI patients were studied between 4d and 4wk post–MI. LV volume index reduced in patients with small infarcts and increased considerably in patients with moderate and large infarcts in 4d-4wk, but filling pressure did not show any noticeable changes. LV dilation is structural and compensatory for increased stroke volume [108]. A similar study demonstrated that LV dilation was still progressive and suffered from declined ejection fraction (EF) and constant stroke volume. This suggests that the dilation is no longer compensatory from 4wk post-MI [109].

MI patients were divided into LV no dilation (38), limited (18) and progressive (14) groups, their LV volume and haemodynamic parameters were observed at 4d, 4wk, 6mth, 1.5 and 3y. Patients with no dilation were in normal LV volume and haemodynamic parameters until 3y. Patients with limited dilation exhibited increased LV volume and depressed stroke volume up to 4wk, but the LV volume was stabilized thereafter, the stroke volume was recovery after 4wk and remained. For the patients with progressive dilation, their LVs were in dilation and the stroke volume was restored by 4wk, but the latter was deteriorated progressively after 4wk [110]. This implies that a sustained LV dilation can result in LV dysfunction.

66 patients with acute MI were underwent LGE CMR evaluation after reperfusion at baseline (1wk), early follow-up(4mth) and late follow-up(14mth) and subject to the reduced mean infarct sizes such as 25±17, 17±12 and 15±11g, respectively [111]. This fact suggests infarct healing is continuous process with the most notable reduction in infarct size within 4mth after reperfusion.

Geometry and hemodynamic changes of LV in 30 patients were monitored on admission and at 2wk after their first acute MI by using echocardiography and catheter to characterise LV remodelling process. The magnitude of remodelling process is directly proportional to infarct size, and the remodelling can improve hemodynamic indexes such as lower LV diastolic pressure and increased cardiac blood output but must be expense of a substantial enlarged LV chamber volume [112].

2.3 Remodelling mechanism

A simple negative feedback model has been proposed by [11, 113] to represent the mechanism for LV remodelling after MI. The mechanism is described by five steps in the following:

(1) after MI, both systolic and diastolic dysfunction occurs due to loss of contractile function of the infarcted myocardium, resulting in a decreased EF, increased LVESV, LVEDV and LVEDP;

(2) peripheral mechanisms are mediated through the sympathetic nervous system and circulating catecholamine maintain a normal arterial blood and cardiac output by altering preload and afterload, leading to an increased LV diameter, LVESP and LVEDP, eventually an elevated ED and ES wall stress as well as progressive dilation and thinning;

(3) infarcted zone is in healing to form firm scar to resist increased wall stress, if the mature scar is unable to resist the elevated wall stress, then LV rupture may emerge;

(4) in non-infarcted zone, high level in wall stress may stimulate volume-overload hypertrophy [113, 114], in consequence, myocyte elongation and wall thickening allow systolic and diastolic wall stress to return to normal level.

A similar but more complicated remodelling mechanism is provided in [3] and no longer repeated here.

2.4 Cellular mechanism for remodelling

LV dilation and thinning during remodelling process has underlying cellular deformation mechanisms. Infarct expansion and thinning are due to decreased number of myocytes and myocyte stretch and reduction of intercellular space of collagen fibres. Remote zone expansion and thinning are caused by side-to-side slippage of myocytes.

The number of collagen fibres per unit area in the wall and the number of fibres between the epicardium and endocardium were measured by using phase contrast microscopy and correlated with the ventricular volume and wall thickness for 8 rats' hearts fixed by glutaraldehyde perfusion. Average interstitial space between fibres (centre to centre separation) was calculated from these measurements. Increasing LV volume is related to decreased wall thickness and fibre diameter, however, the decreases in wall thickness are 3-4 times greater than the decrease in fibre interstitial space, suggesting a dimensional paradox, which may be associated with a mechanism of sliding planes between groups of muscle fibres [115].

The LVs of eight open-chest dogs arrested in diastole at various times (15min, 45min and 2h) after coronary artery occlusion and sarcomere lengths were measured with electron microscope in cardiac wall of ischemic and normal regions [116]. It is found that considerable overstretch appears in the ischemic region immediately after the occlusion because partial disengagement and rupture in the actin filaments of sarcomeres.

To understand the mechanisms of LV wall dilation and thinning, transverse histologic sections of infarcted rat LVs were studied at 1, 2 and 3d after MI. Human LVs from five patients (three died in 3d post-MI and two without coronary disease) were examined histologically in a similar way. In infarct zone, a decrease in the number of myocytes across LV wall contributes most LV wall thinning, and myocyte stretch and reduction of intercellular space accounts for minor wall thinning. In non-infarct zone, myocyte slippage is responsible for all wall thinning [117]. A similar study demonstrated that side-to-side slippage of myocytes was associated with LV dilation and remodelling after MI [118]. If myocytes are lost nearly 40% or more in LV infarct zone, decompensated eccentric LV hypertrophy occurs after MI [119, 120].

The collagen network was examined on the rat hearts obtained at 1, 2, 3, and 4d after MI by using polarized light microscopy. A loss of inter-myocyte collagen struts and a reduction of interstitial space between fibres were found, which is consistent with a mechanism that LV expansion proceeds in terms of slippage of myocytes held by the collagen struts [121].

Twelve sheep LVs were studied before and at 8wk after MI and myocyte volume and length in adjacent to infarct zone were greater than in remote non-infarct zone, but regional intra-myocardial circumferential shortening was correlated inversely with myocyte volume and length in adjacent to the infarct zone [122].

Based on the mouse model, myocyte apoptosis in remote region from MI zone was measured at 1, 4 and 6mth after MI. In myocardium remote from the infarct zone, LV wall was thickened, and myocyte apoptosis was increased, which could be related to LV dysfunction during remodelling [123].

For the pig LV model, at 3wk after MI, non-infarct tissue was remodelled in such a way that it expanded in the fibre and cross-fibre directions simultaneously [124].

2.5 Remodelling intervention

Since LV remodelling after MI may be adverse and can make LV dysfunction eventually. If the remodelling is intervened by using physical or pharmacological methods to alter the remodelling process, then the remodelling can be reverse. Remodelling intervention has been initiated since 1950's and has become a promising and active research area presently.

Thrombolytic therapy is a physical method for limiting infarct size by making infarct artery in patency [125]. Pharmacologic method or intervention potentially minimizes infarct expansion and LV dilation [126-128], angiotensin-converting enzyme (ACE) inhibitor [12,3,127-132], placebo, isosorbide mononitrate, β-adrenergic blockers [11], glucagon [129], and nitroglycerin [5, 127] etc. are commonly used in pharmacologic intervention after MI.

It was shown that remodelling of extracellular collagen matrix (ECM) could play an important role in LV remodelling after MI. In prevention of LV remodelling, protecting ECM during remodelling after MI is an important aspect [132]. Reperfusion and ACE inhibitor can disrupt ECM. Pharmacologic interventions protecting ECM after MI should be a future priority.

Recently, more physical therapies have been developed to relieve remodelling effect after MI by injecting some biomaterials, such as self-assembling peptide nanofibers [14], calcium cross-linked alginate hydrogel [133], alginate and fibrin [134], dermal filler [135], calcium hydroxyapatite-based tissue filler [136,137], hyaluronic acid hydrogel [138,139], collagen [140] or by placing chronic pacing in the MI regions [141] or by removing the infarct region surgically [142] or by supporting LV with constraint device [143].

3 Experimental kinematics of LV

Kinematics of LV is the study on motion characteristics of a LV during cardiac cycles and can be characterised in terms of LV shape, volume, regional function and strain in myocardium. These parameters can be measured by using in vivo techniques, such as MRI, ultrasonography, CT and son on. After MI, the LV shape, volume, regional function and strain vary and exhibit useful features which are potentially utilised in MI clinical diagnosis and remodelling process assessment. On this subject, a large body of literature has been accumulated so far.

3.1 LV shape and its change

Initially, LV shape is described by using Fourier shape-power index. It is also indicated by LV endocardial surface curvature or sphericity index (SI), which is defined as the aspect ratio of LV (the ratio of the short to long axis lengths) in 4CH and 2CH views at ED or ES. The update variables of SI such as apical conicity index (ACI) or apical conicity ratio (ACR) commonly are increasingly adopted to evaluate LV shape, especially in the apex because anterior MI often creates a blunter apex shape. Presently, reconstructed 3D LV-based principal component analysis (PCA) becomes one advanced method for identifying differences in LV shape among patients.

The outer contour of LV in a four-chamber (4CH) image of x-ray contrast ventriculography was fitted with a Fourier series of 8 components, and the Fourier shape power is defined as the sum of the normalized 2^{nd} through 8^{th} component power, which is the sum of the square of sine and cosine amplitudes in each component. It turned out that LV shape could be described more accurately by using Fourier shape-power index rather than circular (Gibson) shape index and eccentricity for normal LVs and the LVs in patients with aortic and mitral valvular regurgitation [144].

The LV wall thickness in six regions in short-axis view images of the rats was measured at 1, 2 and 3d and it was found that wall thinning extent and increased radius of curvature in the MI zone with expansion were independent of infarct size [145].

Curvature at any point on the endocardial contour of 4CH ED and ES echocardiaograms of 68 patients with anterior MI at 24h and 1y post-MI was calculated and compared with that in normal LVs. It was indicated that curvature analysis can identify the geometrical changes induced by MI [146].

Large infarct was created in the rat LVs, and ED and ES volumes were measured, and diastolic and systolic stresses in LV wall were estimated with ellipsoidal model [147]. LV

circumferential radius of curvature is increased in remote region, but LV longitudinal radius of curvature is enlarged in the whole LV, while the apical sphericity is increased substantially based on MRI tagging results of sixteen patients with reperfused anterior MI at 5d [148]. The large infarct led to increased ED and ES volumes and wall stresses, especially, a change of the LV from ellipsoidal to cylindrical. It was shown that increasing LV SI as an independent predictor of decreased 10y survival rate after MI [149].

MI can make a geometrical change near LV apex, but LV sphericity index is unable to identify this change. Hence ACI was proposed to quantise the geometrical change near the apex. ACI is defined as the ratio the diameter of a circle by which the endocardial contour near the apex is best fitted to the short axis length in 4CH view. It was shown that ACI of LVs with anterior infarction was different significantly from normal LVs while SI remained the same, especially, in the case where anterior MI resulted in a less conical or blunter apex shape [150].

Likewise, ACR, which is the ratio of the area of apex surface to the area of apical triangle in 2CH view, was proposed to evaluate the apical geometrical alternation induced by MI. For LVs with aneurysm after MI, ACR differed significantly from normal LVs, but SI and ACI showed little variation [151].

Based on long-term clinical and echocardiographic results of LV dilation treatment post-MI, the strategy of emphasis on LV shape rather than on LV volume can lead to a better survival probability after the LV surgery [152,153].

To identify differences in remodelling process between ischemic cardiomyopathy (ICM) and global non-ischemic cardiomyopathy (NICM) for patients with anterior MI, LV geometrical models at ES and ED were built from multi-detector computed tomographic (MDCT) images, and the difference in LV shape between current LV configuration and averaged LV configuration was decided by using PCA [154]. PCA coefficients could capture significant LV shape difference at ED and ES and PCA method is feasible to quantify regional shape differences at ES during MI remodelling process.

PCA was applied to derive remodelling model based on MRI atlas of 300 patients with MI images [155]. Twenty shape models at the end of diastole and systole were determined by using logistic regression, the progression of MI over time, and effects of treatment were captured.

The LVs of eight patients with aneurysms after MI were reconstructed based on fast cine-angiographic computed tomography slices at ED and ES and LV wall thickness, curvature and stress index were calculated [156]. According to the wall thickness and curvature, aneurysmal, border and remote zones were specified. The stress level/index increases from the remote zone to the aneurysm.

Border zone geometrical feature was measured by using 2D [157] and 3D [158] echocardiography on a few sheep LVs after acute MI. Decreased wall thickness and curvature in the border zone after MI were observed. These two effects can raise the wall circumferential stress level by 12% [157].

3.2 LV chamber volume and pressure

LV chamber volume includes end diastolic volume (LVEDV) and end systolic volume (LVESV) and EF, LV chamber pressure involves end diastolic pressure (LVEDP) and end systolic pressure (LVESP). These characteristic volumes and pressures represent LV pumping function and can be altered post-MI. Usually, the larger the LV chamber, and the higher LVEDP, the more the LV pumping function is impaired. LVESV is an excellent predictor of survival after MI in comparison with EF and LVEDV. The changes in LVEDV, LVESV and EF between 5mth and 4d after MI can be used to classify remodelling types. LVEDP is increased post-MI, and patients with LVEDP >30mmHg will suffer from the highest possibility of death or heart failure.

LVs of 125 patients were examined by electrocardiography after the first acute MI at 2, 6, 12mth, 5 and 7y [159]. At 5y of follow-up, 68% of patients with normal sized LV were alive compared with 47% of patients with enlarged LVs. This suggests that the mortality of the former is 32% in comparison with 53% in the latter.

Based on the dog model, LVEDP was measured at various MI sizes. LVEDP increased from 7mmHg to 20mmHg with increasing MI size, and stroke index decreased from 30 to 20ml/beat/m^2 approximately with increasing LVEDP [160].

The distance from the midline of the LV border, i.e. external left heart dimension (LHD) was measured on roentgenograms serially in 125 patients after MI at baseline, 24h, 2d, 2wk, 2, 6mth, 1.5 and 2y etc. The mortality of patients with enlarged LVs was 26% at early stage (<4wk) compared with 4% with normal LV size. At late stage (>4wk), the mortality was 24% in comparison with 8% with normal LVs [161]. This fact indicates LHD is a useful predictor of survival and mortality post-MI.

LV function of 19 closed-chest dogs was measured at 3-4wk (early stage of scar formation) and 6-8wk (late stage of scar formation) after MI. In both the early and late stages, the infarcted LV had normal LVEDV and normal isovolumetric velocity-force length relationships but elevated LVEDP as well as reduced velocity of shortening during ejection [162].

LVEDV, LVESV and EF of 49 patients in 2-12mth after MI were determined by biplane ventriculography and heart size was calculated from chest films by using cardiothoracic ratio (CTR) and cardiac volume (CV) methods. There is a linear relation between LVESV and LVEDV and a hyperbola relation between EF and LVEDV, respectively. The smaller the LV chamber size (<150ml/m^2), the wider range the LV function; but the larger the LV size, the more severe the LV dysfunction (EF<0.3) [163].

Impairment of LV function was quantitated by measuring LVEDV, LVESV, EF and severity of coronary arterial occlusion and stenosis in 605 male patients at 1 to 2mth after a first or recurrent MI and the survivors of these patients in 15-165mth [164]. It was demonstrated that LVESV is the primary predictor of survival after MI than EF and LVEDV.

LV volume of fifty-seven patients in the convalescent period of acute MI was measured by making use of radionuclide method at 2wk and around 1y post-MI, and the median end-diastolic volume index increased from 90 to 112ml/m^2, the median end-systolic volume index from 51 to 61ml/m^2 and median stroke index from 39 to 47ml/m^2. The patients with anterior MI exhibited more dominant increase in those parameters and were at significant risk of heart failure [165].

Biplane diastolic circumference and contractile and non-contractile segment lengths were measured using biplane ventriculography in 52 patients with anterior MI at 3wk and 1y post-MI. Further, LV global geometry was assessed with SI and regional geometry was evaluated with endocardial curvature [166]. LVEDV increased from baseline to 1y due to increasing contractile segment length and SI, but the non-contractile segment length decreased. The anterior-basal, inferior and margins of the MI became flattening, and the anterior wall showed a less bulging. LV enlargement after MI is caused from an increase in contractile segment length and a change in LV geometry rather than from progressive MI expansion.

Based on 2D transthoracic echocardiograms of 412 patients at mean 11.1d post-MI and of 420 survivors at 1y, LV cavity areas at ED and ES were obtained and LV function was assessed in terms of percent change in cavity area from end diastole to end systole [167]. Baseline LV systolic area and percent change in area were strong predictors of cardiovascular mortality and adverse remodelling.

A LV dilation model after MI was proposed in [168] based on LVEDV and LVESV. In the model, LVESV and LVEDV at any time after MI can be calculated by an exponential function of LVEDV index and LVESV index as well as time along with six regression coefficients. LVEDV index is composed of LVEDV of baseline or LVEDV at 3d post-MI, male gender, peak CPK; similarly, LVESV includes these parameters but LVESV of baseline or at 3d after MI. The high risk LVEDV, LVESV and LVEDV+LVESV indices at 6mth post-MI are 63, 30 and 88ml/m^2, respectively.

LVEDP is an essential measures of LV performance and may discriminate patients at increased risk for developing heart failure after acute MI. LVEDP of 744 acute MI patients over 36mth post-MI were analysed in [169]. It was shown that the mean LVEDP is 23±9mmHg and 75% of patients with an LVEDP being higher than 15mmHg; especially, patients with an LVEDP>30mmHg were at the highest risk of death or heart failure.

Images of cine MRI and LGE of 46 patients within 7d following primary percutaneous coronary intervention for acute ST-elevation myocardial infarction (STEMI) with follow-up at 1y were taken and co-registered and local LV dilation was assessed [170]. Local LV remodelling between baseline and follow-up (percentage of LV expansion) within MI region was greater than in non-infarcted myocardium.

MI can cause LV adverse remodelling, i.e. LV enlargement and dilation to result in heart failure and mortality. Potential thresholds of LV remodelling were identified based on the murine model by using MRI with LGE in [171]. MI size >36% at 2d after MI is the best single predictor for

adverse remodelling at 30d, and LVESV >32ml is an excellent predictor, too. Further, the combined two factors can achieve the highest predictive values for the adverse modelling at 30d.

The changes in LVED, LVESV and EF of 40 reperfused STEMI patients, i.e. ΔLVED, ΔLVESV and ΔEF between 5mth and 4d after MI were determined by using CMR, and cut-off values for ΔLVED, ΔLVESV and ΔEF to well predict EE<50% at 5mth in 146 reperfused STEMI patients were obtained [172]. By using 12% of both ΔLVED and ΔLVESV, four important patterns of LV remodelling are identified, namely, reverse remodelling, no remodelling, adverse remodelling with compensation and adverse remodelling as shown in Fig. 3.

3.3 LV regional function

LV regional function is the local contracting ability of myocardium in MI, border and remote zones, respectively, post-MI. This issue came to be noticed since 1970's. The regional function is usually in terms of segmental shortening of myocardium which can be obtained experimentally only. The segmental shortening of myocardium is measured by using sensors implanted in LV wall traditionally in vitro; the best way for measuring the segmental shortening is in vivo MRI tagged currently. It was shown that a difference in segmental shortening in both the circumferential and longitudinal directions between border and remote zones exists from 1wk to 6mth post-MI. Since experimental data are very in shortage, quantitative conclusions cannot be achieved presently.

The relationship of abnormal regional myocardial performance to LV function 1-12mth post transmural MI was established by identifying abnormally contracting segments (ACS) of 24 patients with biplane angiocardiography in [173]. The patients with heart failure had a very low EF (<0.30) and a quite larger ACS (>23%) where ACS was expressed as a percentage of the LV circumference at ED. EF and LVEDP could be correlated to ACS with quadratic and linear regression equations, respectively.

Regional myocardial function was observed by using ultrasonic dimension gauges in open-chest dogs after acute coronary artery occlusion. In the ischemic segment, an instant systolic dysfunction was observed and end-diastolic segment length (EDL) was reduced by 11%, segment stroke work was smaller by 91%, and diastolic pressure-length curve was moved and steepened. In the margin segment, active shortening and stroke work were decreased by 37%, but the EDL increased by 4%. In the remote/control segment, active shortening increased, followed by compensatory operation of the Frank-Starling mechanism [174,175].

Regional myocardial function was studied by checking LV EDL changes with pairs of ultrasonic gauges and a micro-manometer implanted in the sub-endocardium of the dog LVs in 4wk from MI occurrence [176]. Correlations were found between EDL and EDL shortening. Hyper-function in normal regions and variable segmental loss of contractile function along with reduction of sub-endocardial dimensions were presented.

Under anterior-apical infarct condition for the sheep, MRI tagged images in short-axis and long-axis were obtained before and 1, 8wk and 6mth after infarction [177]. A difference in circumferential and longitudinal segmental shortening between adjacent and remote healthy myocardium occurred at 1wk and existed up to 6mth. This difference is responsible for LV cavity dilation, eccentric hypotrophy and lengthening of non-infarcted segment during LV remodelling.

The difference in regional function of infarcted LV is related to reduced LV systolic wall thickening in the central MI zone and increased systolic wall thickening in remote [178].

For 25 acute LV patients, the remote myocardium demonstrated reduced systolic thickening of dysfunction/ECM expansion within one week after MI [179], such expansion is coupling with infarct healing.

3.4 LV myocardial strain and growth strain

LV myocardial strain is the LV wall strain in a cardiac cycle when a LV at end-diastole or end-systole is referred to be reference configuration. LV growth strain is the strain at end-diastole or end-systole at a late date when the LV at another early date is used as reference configuration at the same end of cardiac cycle. The myocardial strain demonstrates the deformation in LV wall during a cardiac cycle, but the growth strain specifies the deformation caused from LV mass growth over days or months or even years.

3.4.1 Myocardial strain

Myocardial strain has been measured by tracking radiopaque markers implanted in LV walls in vitro since 1990's. Currently, MRI tagged with LGE has become the major in vivo method for strain measurements. The principal strains and their orientation vary from MI zone to border zone (BZ) and remote zone, their magnitudes reduce during remodelling process. It is interesting that peak systolic longitudinal strain is a good predictor of adverse remodelling and reverse remodelling. The derivatives of circumferential and longitudinal strains with respect to time, i.e. circumferential and longitudinal strain rates are a predictor of heart failure.

Rat LV 2D strains were measured on infarcted LV's surface with a triangle of white dots at the mid-ventricle with titanium oxide powder at 2wk after MI. It was shown that the passive loading strains are smaller in the MI zone along the collagen fibre and cross-fibre directions, and the collagen fibre tortuosity decreases with LV pressure in the MI and remote zones but not significant, suggesting that collagen fibre structure in the MI zone may be different from that in the remote [180].

Mathematical modelling tools were developed to obtain 3D strain field in the posterior, lateral and septal walls in LVs of the mice based on MRI tagged images with LGE at baseline, 1, 7 and 28d post-MI. For the principal 3D contraction strain, permanent dysfunction in the MI zone, intermediate function in the BZ and maintained function in the remote zone are exhibited, respectively [181].

In seven sheep, 3D deformation of their LVs was tracked by tissue tagging in short- and long-axis planes with MRI, the principal strains and systolic in-plane translation and rotation were calculated. The magnitudes of the 1st and 2nd principal stains are reduced in both the planes at 1wk after MI and the principal directions also vary [182].

Regional epicardial strain profiles were measured by using radiopaque markers in the canine LV with MI, and the BZ for fibre strain is quite narrower than that for cross-fibre strain and considerably wider for LAD coronary occlusion than LCX coronary occlusion [183].

Based on the porcine model, principal systolic strains were calculated from the strain components of MRI 3D tagged sequence in infarcted region, BZ and remote zones at baseline, 1wk, and 4wk after MI [184]. The maximum and minimum principal strain magnitudes were lowered with remodelling in progress.

Another piece of ultrasound study showed that both longitudinal and circumferential strain rates are predictive of heart failure, and circumferential strain rate can strongly predict LV remodelling at 20mth [185]. However, another piece of work showed that peak systolic longitudinal strain respectively with cut-off thresholds, such as -(12.8-10.2)% and -(13.7-9.5)% can predict adverse remodelling and reverse remodelling accurately based on a meta-analysis on 3066 MI patients [186].

3.4.2 Growth strain

Growth strain is measured by tracking 0.7-1mm diameter gold beads implanted in LV walls in vitro with biplane cineradiography or video-fluoroscopy presently. Since such measurements are few, a consistent conclusion from them is hard to be reached. Basically, the radial systolic growth strain is more significant than the circumferential and longitudinal strains, and the latter two are comparable in magnitude from 3wk onwards after MI.

Three columns of four to six gold beads in 1mm diameter were implanted in the LV anterior free wall in five dogs and bead positions were tracked before and after LV enlargement induced by creating a systemic arteriovenous fistula [187]. Continuous ED transmural growth strain distributions were gained by fitting the three columns of the bead with the edges of single bilinear-quadratic finite elements. Growth strain was calculated from the ED control configuration to the ED hypertrophy configuration. The distributions of the circumferential and longitudinal components of the strain were uniform and positive. Since the radial growth strain was small, growth was significantly parallel to the epicardial tangent plane was suggested. The in-plane fibre and cross-fibre components of the growth strain were positive across the wall with nearly equal in magnitude, thus growth in the cross-fibre direction was substantial.

Gold beats were implanted in the LV free wall of five pigs and were tracked by using biplane cineradiography to reconstruct the 3D deformations of the myocardium in single cardiac cycle and the remodelling deformations presented at 1 and 3wk [188]. Systolic strains were determined by end

diastole of a given cardiac cycle as the reference configuration and end systole of the same cycle as the deformed/current configuration. However, remodelling strains were calculated by specifying end diastole at one time as the reference configuration and end diastole at later time as the current configuration. There was permanent loss of systolic strains at 1wk, but large shears at 3wk in the infarct region. The remodelling circumferential strain was the largest and the radial strain was the smallest but the longitudinal one was in between in magnitude at 1wk. At 3wk, the radial strain was the most dominant, and the longitudinal strain was the shortest (near zero), while the circumferential strain was in between in magnitude.

Three transmural columns of four 0.7mm diameter bead sets each were implanted across the mid-lateral equatorial region wall of a sheep LV and bead images were recorded using biplane video-fluoroscopy after MI at 1wk and 8wk [189]. Systolic strains and remodelling/growth strains were calculated by fitting beat displacements with finite element method. The lateral LV wall, which is adjacent to the MI, grown longitudinally by more than 10%, thinned by more than 25% and lengthened circumferentially by more than 5% at 8wk.

4 Experimental kinetics of LV wall

Kinetics of LV is the study on relationships between force and motion in LVs. A LV must be expanded passively to be filled by the blood from the pulmonary artery, but also contract actively to discharge the blood into the aorta. The biomechanical properties of LV myocardium include passive and active behaviours, and usually can be described by using force-velocity relation, stroke work-LVEDP curve, end-systolic *p-V* relation, diastolic *p-V* curve, pressure-length relation, stress-strain curve, relaxation or creep curves and rupture threshold.

4.1 Force-velocity relation

Force-velocity relations are the application of the well-known Hill three-element (i.e. contractile element, series elastic element and parallel elastic element) force-velocity equation for skeletal muscle in shortening [190] into a piece of cardiac muscle or an intact LV. A series of pioneer work on this topic can be found in [191-194] for the cat right ventricular papillary muscle and [195] for the rabbit papillary muscle as well as [196-201] for the dog healthy intact hearts in vitro based on thin-walled spherical LV model.

Notably, the acute cardiac failure induced by pentobarbital or pronethalol in the dog LVs can reduce the extent of circumferential fibre shortening by 30% in average [202]. The relationships of velocity of shortening with isovolumetric pressure were extracted based on spherical LV model and the assumption that contractile element velocity was equal to the series elastic elongation in terms of 8 patients in [203]. The instantaneous isovolumetric velocity of shortening during the isovolumetric contraction is expressed by

$$V_{ce} = (dp_{iso}/dt)/(k_1 p_{iso}) \quad (1)$$

where V_{ce} is the velocity of shortening, p_{iso} is the LV pressure during the isovolumetric contraction, k_1 is the series elastic constant, k_1=2.5mm^{-1} for the cat right ventricular papillary muscle [204]. The maximum velocity of shortening has been attempted to correlate with various heart lesions [205,206].

Effects of acute regional MI on LV pumping function were identified by using the thin-walled spherical LV model based on 40 anesthetized dog LV models, and it was shown that the isovolumetric force-velocity curve of the same dog LV during coronary artery occlusion is shifted downwards and to the left in comparison with before the occlusion at the same LV volume [207]. This implies that LV wall will generate a smaller active tension during coronary artery occlusion than before the occlusion at the same LV volume.

4.2 Stroke work-LVEDP curve

Stroke work (SW) is defined as the integral of LV pressure with respect to LV volume in a cardiac cycle, i.e.

$$SW = \oint pdV \tag{2}$$

in reality, however, *SW* is commonly estimated by making use of mean LV pressure $\bar{p}$ in ejection, LVEDP and LV stroke volume (SV). The expression for SW estimation is written as [199]

$$SW = SV \times (\bar{p} - LVEDP) \tag{3}$$

It was shown that the SW-LVEDP curve of the LV with MI rises as LVEDP increases and is shifted to the left with a smaller slope compared with that in the healthy dog LV [202].

4.3 End systolic *p-V* curve

Usually, end systolic *p-V* or LVESP-*V* relation is the *p-V* curve at ES. The curve represents the residual LV chamber volume and pressure after a LV finishes its systolic stroke, and is independent of loading conditions. A large residual LV chamber volume and a high pressure mean a poor LV pumping function. Thus, the curve can assess LV contractile/pumping function explicitly. MI alters the volume intercept of a LVESP-*V* curve more considerably than does the slope of the curve. Additionally, the curve moves rightwards in comparison with that before MI occurs, depending on MI size, collagen content and LV dilation.

The end systolic *p-V* relation of seven chronically instrumented dogs was measured in vitro when circumflex coronary artery occlusion occurred [208]. It turned out that the end systolic *p-V* data of each dog can be best fitted by the following linear relation before and after coronary artery occlusion

$$p = E_{es}(V - V_0) \tag{4}$$

where p is LV end-systolic pressure, V is LV end-systolic volume, V_0 is the volume intercept of the end systolic *p-V* relation, and E_{es} is the slope of the relation. Before occlusion, the means of slope and intercept of seven dogs are E_{es} =6.9 $\pm$ 2.1mmHg/ml and V_0 =10.1 $\pm$ 7.8ml, while they are E_{es}=6.7$\pm$2.6mmHg/ml and V_0=20.4$\pm$9.8ml after occlusion, showing V_0 is statistically significant

before and after occlusion(P<0.005) [208]. A similar conclusion can be found in [209]. This fact demonstrates that MI affects mainly on the volume intercept and the LVESP-V curve exhibits a rightwards shift phenomenon.

As a further investigation of [208], the change rate of LVESP with time is obtained by taking the first derivative of p with respect to time t, namely

$$dp/dt = (dE_{es}/dt)(V - V_0) \quad (5)$$

and the maximum derivative dp/dt_{max} was identified. It was indicated that occlusion of LV LCX coronary artery can induce a rightward shift of the dp/dt_{max}-volume curve with an increased volume intercept of 11.3±5.3ml compared with the normal condition[210].

More recent work demonstrated that the existence of healing MI scars can alter the end systolic *p-V* relationship to shift rightwards and to impair systolic LV function at 1, 2, 3 and 6wk after MI in the infarcted rat LVs [92], depending on MI size, collagen content and LV dilation.

The global active stiffness in intact LV in anesthetized dogs was measured in vitro after MI at 1h and 2-3wk by using three methods. In these MI periods, the global active stiffness of LVs varied, but markedly reduced after scaring and thinning were completed [211].

4.4 Diastolic p-V curve

Diastolic *p-V* curves represent LV diastolic function. A large LVEDV and a low LVEDP mean a better LV diastolic function. MI can change the *p-V* curve position and shape. Usually, a LV *p-V* curve moves to the left as soon as at 1h after MI with an increased stiffness or a reduced compliance compared with the normal LV. After 3d post-MI, the curve gets normal. The *p-V* curve shape is described by the curve slope-stiffness or its reciprocal-compliance. Diastolic *p-V* curves can be expressed mathematically with an exponential function and the slope dp/dV has a linear relationship with p, the slope of a linear $dp/dV - p$ curve rises after MI, suggesting MI makes a diastolic *p-V* curve stiffer.

LV systolic function was studied by using the curve of LV developed pressure as a function of LVEDP in eight intact conscious dogs before, at 1h and 6-8d after MI during transient aortic occlusion with balloon catheter [212]. The LV developed pressure is defined as the difference of LV peak systolic pressure minus LVEDP. The LV function curves were depressed greatly at 1h post-MI but showed a recovery trend towards the control at 1wk.

Post-mortem *p-V* curves and pressure-length curves were measured in the dogs at 3-5d after MI. The length of infarcted and remote regions was obtained by using mercury-in-silastic segment length gauges. Post-mortem *p-V* curves exhibited reduced compliance in comparison with the normal LV. The compliance of the pressure-length curves in the MI zone was higher than the remote zone, while the compliance of pressure-length curves in the remote zone was nearly identical to that of the normal LV [213].

LV wall compliance was assessed by calculating the compliance (dV/dp) of diastolic p-V curves measured in vitro in eight normal dog LVs and in five LVs at 1h after MI. The mean p-V curve of five LVs after MI was shifted to the right of the mean curve of eight control LVs. As a result, the compliance increased to 17.54ml/mmHg from 10.10ml/mmHg [214]. For the rat model, a similar result at 26d after MI was identified as well [215].

After experimental infarction in dog models was created, diastolic stiffness was increased by 21%, and isovolumetric relaxation was slowed by 51% in terms of the minimum slope of diastolic pressure-time curve [216].

The p-V curve of a LV is usually an experiential function of p, thus the LV wall stiffness is expressed with a linear relationship

$$dp/dV = ap + b \tag{6}$$

where the slope of this function a was called the passive elastic modulus/stiffness. Based on LV catheterization data after MI at 2-25h, a=0.005 for normal LVs, a=0.011 for 13 patients with coronary artery disease, and a=0.045 for 12 patients with acute MI. A further increase in wall stiffness was observed with the development of acute MI, 87% patients with 0.5mmHg/ml wall stiffness or 2ml/mmHg wall compliance died of power failure during the acute stage of MI [217].

Diastolic p-V curves of the rat LVs were measured ex vivo at 3, 24h, and 3, 5d, and more than 22d after MI. Before 3d, the diastolic p-V curves moved to the left of the normal LV and gets stiffer; at 3d, the p-V curve is restored to the normal curve; but after 3d, the curves are shifted to the right of the normal curve, showing a less stiff trend [218], as shown in Fig. 4.

p-V loops were measured in vivo by using colour echocardiography and catheter at 6wk in rabbits post-MI and sham. The loop at 6wk showed a larger early diastolic volume and higher early diastolic pressure, but a lower systolic pressure and a larger LVESV compared with the loop of the sham [219].

4.5 Pressure-length relation

Pressure-length curves are the curve of LV chamber pressure against the segmental length of two gauges implanted in LV walls in a cardiac cycle. Based on the pressure and the LV spherical membrane mechanics model, i.e. the Laplace's law, the tension in the LV wall can be worked out, eventually, the tension-length curves become available. Such a representation of LV kinetics is popular in 1970's only and it has been replaced with stress-strain relations presently. It was demonstrated that diastolic pressure-length curves were shifted to the right and the tension in LV wall can be expressed with an exponential function of segmental length.

Typical systolic and diastolic tension-length curves of cardiac wall were provided in [200] as ischemia occurred in the anterior descending coronary artery during both diastole and systole based on the dog model. It was illustrated the systolic tension-length curve goes down significantly in the

ischemia state from the normal state, but the diastolic tension-length curve remains unchanged basically.

LV myocardial segment lengths were measured by using an epicardial mercury-in-sliastic gauge and LV pressure-length loops were presented before and after anterior descending artery occlusion in 11 dogs. It was shown that LV systolic function was deteriorated rapidly after occlusion in terms of the pressure-length loop area, and the ED pressure-length curve was shifted to the right, exhibiting increased diastolic compliance [220].

Serial in situ measurements of segment length were carried out by employing mercury-in-sliastic gauges sutured directly to the LV surface of dog at 1h and 6h after MI in one cardiac cycle, and the LV function was presented by using LV pressure in terms of normalized segment length-muscle length which was defined as the ratio of the phasic segmental length to the ED segment length. The pressure-muscle length curves at 1h and 6h after MI all move to the right of the curve of the control and the ED muscle length is the maximum at 1h after MI and the minimum in the control, while the length at 6h post-MI is in between [221], as shown in Fig. 5. At 6h after MI, LV wall losses contractile function and the slope of passive pressure-length curve became stiffer compared with the control [222].

Regional segmental motion after MI in seven dog LVs was measured by employing a pair of ultrasonic crystals implanted in LV wall during the withdrawal of 500ml of blood and the transfusion of 800ml of blood, and the tension in LV wall was estimated by using the Laplace's law for a simple spherical membrane model [223]. The tension-length curves after MI were moved to the right compared to the control case, the blood withdrawal and transfusion allowed the tension-length curves to shift to the right even further. The relationship between tension and length of LV segment is exponential, such as

$$T = exp[10 \times a \times (L/L_0) + b] \quad (7)$$

where T is tension in LV wall, L is the instantaneous length of a MI segment and L_0 is the length at ED before MI occurs, a and b are the parameters fitted by using tension-length scattered data.

4.6 Uniaxial stress-strain curve

Uniaxial stress-strain curve is the stress-strain curve of a specimen of myocardium in uniaxial elongation in passive state. For isotropic materials a uniaxial stress-strain curve represents the material constitutive law exactly. For anisotropic materials like myocardium, uniaxial stress-strain curves in multiple direction are required. For myocardium with MI, experimental uniaxial stress-strain curves are rather lack. It was indicated that uniaxial stress-strain curves of myocardium with MI are exponential in terms of strain, the exponent in the curves is constant in remote zone and varies a little in 10d after MI.

Specimens from the infarcted region of the LVs in 58 rabbits killed were harvested at 4h and 1, 2, 5, and 10d after MI, and the stress-strain data were obtained after the specimens were elongated simply [224]. Based on the exponential constitutive law

$$d\sigma/d\varepsilon = k_2\sigma + c \tag{8}$$

for soft bio-tissues in [225], the data points of stress-strain curves were best fitted and the parameter k was plotted versus time after MI. In remote zone, it is k_2=10.6, and there is no significant variation in k_2 over 10d in MI region [224].

Isolated strips of rabbit myocardium from acutely ischemic (non-infarcted), acutely infarcted (24h after MI) and healed infarct (3wk and 5wk post-MI) zones were repeatedly stretched under a cyclical load with amplitude 2.0g/mm^2 (afterload under LV physiological condition) or 0.2g/mm^2 (preload under LV physiological condition) for 1h at 4Hz. Under the preload condition, the produced elongation was so very small that it was reversible with strip unloading. Under the afterload condition, the elongation was irreversible in acutely ischemic tissue and 15wk-old scar, implying the stress in MI region could influence LV geometry and remodelling post-MI [226].

4.7 Biaxial force-extension curve

Biaxial force-extension or stress-stretch or stress-strain curves of myocardium in passive state are the relationship of force or stress with extension or stretch or stain measured under the condition where a squared planar specimen is elongated in two in-plane directions simultaneously on a material testing machine. The curves specify the in-plane anisotropic property of the myocardium specimen. The passive biaxial property of myocardium is better approximate to the true passive biomechanical property of myocardium than the passive uniaxial property does. However, the extension ratio between two directions during stretching can affect the tested results, and how to select the ratio to mimic the physiological condition of myocardium is tricky. The experimental data points are related to each other in two directions in biaxial tensile tests. If published experimental data are presented in curves, they hardly can be used to develop a constitutive law because the data points in two directions recorded at same time moment are not identified in curve digitization process unless they are listed in a table. Existing biaxial experimental data of myocardium with MI are a few. Basically, the stress in MI and remote regions is in peak at 1wk then is reduced. MI scar at 3wk post-MI is nonlinear and isotropic.

Biaxial force-extension measurements were performed on squared specimens freshly harvested from remote, non-infarcted and infarcted myocardium in sheep LVs before and 4h, 1wk, 2wk and 6wk after MI. In the infarct myocardium, Cauchy stresses at 15% extensions increased in 4h, peaked at 1-2wk, and then reduced in MI region at 6wk after MI, see Table 1. For the stresses in the remote zone, a similar time course occurred in lesser extent than the infarcted region, and collagen content was unrelated to infarct stiffness but increased after 6wk [227].

Infarct scar samples (10-15mm per side, 1-2mm thin) harvested from rat LVs wall at 3wk after MI were stretched by using biaxial testing device [92]. Since the collagen fibres have not exhibited a preferred orientation at 3wk, an isotropic nonlinear homogeneous constitutive law is proposed as the following to fit the experimental stress-stretch data [92]

$$\psi = c\left(I_1 - 3\right)^2 \tag{9}$$

where ψ is the strain energy density function, c is model constant determined from the experimental stress-stretch data, I_1 is the first invariant, I_1=tr($\mathbf{C}$), $\mathbf{C}$ is the right Cauchy-Green deformation tensor, $\mathbf{C} = \mathbf{F}^{\mathrm{T}}\mathbf{F}$, $\mathbf{F}$ is deformation gradient tensor, $\mathbf{F}^{\mathrm{T}}$ is the transpose of $\mathbf{F}$.

In [135], the circumferential and longitudinal specimens of infarct myocardium of sheep LV at 8wk after injecting calcium hydroxyapatite-based tissue filler in 3h post-MI were stretched on a biaxial testing machine, durable infarct thickening and stiffening were observed.

4.8 Viscoelastic property

Viscous property of soft tissue is the viscous resistance to stretch in passive or active state. Such a property in small bundles of cardiac muscle harvested from the apex and base of a ventricle was identified in 1940's [228]. Since 1960's this property has been clarified in detail by employing papillary muscle of mammalian animals under varying experimental conditions, namely cyclical loading, variable strain rate, creep and relaxation [228-234].

4.8.1 Basic viscoelastic model of healthy LV

Based on 13 healthy dog intact LV models, the diastolic pressure-circumference curves were obtained in stepwise haemorrhage and transfusion of blood, the viscosity and inertia of LV wall could alter the curves to some extent, showing a viscoelasticity in the wall during diastole [235]. Subsequent experiments identified that filling rate [236] and heart rate [237,238] could influence the diastolic pressure-volume curve. The viscoelastic properties of normal LVs of 15 conscious dogs were investigated under acute increasing systolic and diastolic loading conditions by establishing the relationships between circumferential stress and natural/logarithmic strain in terms of ellipsoidal shell model in [239]. The static stress-strain curves were obtained by fitting the stress-strain data points in diastasis by using exponential function. It was shown that the short-term series viscous properties due to dynamic loadings were negligible, while parallel viscous property was significant and could be modelled with a function of strain rate, the total stress is estimated by the following relationship [239]

$$\sigma = \alpha\left(e^{\beta\varepsilon} - 1\right) + \eta\dot{\varepsilon} \tag{10}$$

where σ is the circumferential stress, ε is the circumferential natural strain, $\dot{\varepsilon}$ is the strain rate, α, β are the property constants of the static stress-strain curve, and η is the parallel viscous property constant, i.e. the viscosity. For the normal LVs of the dog, the viscous properties were nonlinear and increased

with circumferential length, but also related to incomplete ventricular relaxation in early diastole [240].

In patients with congestive cardiomyopathy [241] and hypertrophy [242], the stiffness β and viscosity η are increased compared with normal LVs. For the dog model, the stiffness β is normal in partial, but increased in complete coronary occlusion [243].

4.8.2 Viscoelastic property of LV with MI

Eq.(10) with η=0 has been applied to investigate effects of global ischemia on the diastolic properties of LV in the dog in vitro [244]. It was shown that the diastolic mid-wall circumferential stress-strain curve shifted upwards and to the left with ischemia, suggesting a decrease in LV chamber compliance in the diastolic *p*-*V* relationship.

Scar tissue strips were stretched to obtain their elasticity based on the rabbit model to identify effects of early reperfusion and late reperfusion on post-MI healing by applying 4Hz phasic physiological stretch or continuous stretch as illustrated in Fig. 6 [245]. The 4Hz phasic physiological stretch was approximate to 200-300beats/min with a peak LVESP of 180mmHg. The viscoelastic properties of the scar tissue were examined by stress relaxation, i.e. the time-dependent decrease in force of the scare specimen held at a constant strain, and creep, i.e. the time-dependent elongation of the scar specimen held a constant force.

Reperfusion at 1h after MI does not influence scar tensile strength measured at 1wk post-MI, but reduces the strength measured at 3wk, see Fig. 7. The tensile strength of the scars with reperfusion at 3h post-MI is quite lower than that of the scars with non-reperfusion due to significant low collagen content in the former. Myofibre holds the minimum tensile strength in comparison with the scar tissue.

The stress-strain curves and tangential stiffness *k*-stress curves are illustrated in Fig. 8. The stress-strain curve of the scar tissue with reperfusion at 3h post-MI is the stiffest, and the curve of the healthy myocardium is the softest, the rest curves are in between.

Effect of reperfusion on viscoelastic properties at 3wk after MI is shown in Fig. 9. Stress relaxation is in terms of % decrease in stress from an initial stress level of 3g/mm^2 at a length held for 5min, but creep is expressed by % increase in length in 5min at a constant stress of 3g/mm^2 applied. The scar tissues exhibit more significant stress relaxation, but less creep effect compared with the healthy myocardium. The viscoelastic properties of the scar tissues are affected less by reperfusion.

4.9 LV rupture threshold

Cardiac rupture is a complication of acute MI. The incidence of the rupture can cause immediate death at a rate of (4-24)% in all infarction deaths [246]. Most rupture is related to anterior MI (55%), and posterior MI (47%) [247] and typical rupture site is illustrated in Fig. 10. The LVs with rupture were with more narrowing coronary artery in comparison with the patient group without rupture [247].

Rupture threshold is important to assessment of rupture occurrence, and usually is measured in vitro. For intact LVs, LV chamber pressure at rupture can be used as rupture threshold. For myocardial strips, the tensile strength and strain at rupture can serve as rupture threshold. The rupture threshold of normal LV myocardium is lower than MI scar tissue in terms of tensile strength. Tensile strength at rupture varies across LV wall, but strain doesn't. Reperfusion doesn't affect rupture threshold. Rupture threshold may depend on age of MI, but existing experimental results are inconsistent.

Collagen formation and mechanical resistance of infarcted LV to stretch and rupture were measured in 36 rabbits from 1d to 8d after MI, and the rupture pressure (644mmHg) in the infarcted LV was not remarkably different from that of the healthy LV on days 1-8. LV rupture occurred more frequently on days 1-4 (59%) than on days 6 and 8 (18%). Wall stress at the point of rupture in normal LVs was 30g/mm^2, for the scar strips at 7d, was 59g/mm^2 [248].

Rupture threshold was measured by using balloon technique in 26 dog LVs without infarction and 44 dog LVs with anterior infarction 1d-6wk after MI. Rupture threshold in non-infarcted LVs was higher than in infarcted LVs. Rupture threshold in infarcted LVs depended on time after MI, for example, the rupture threshold decreased after 2wk, and the mean threshold for 3-6wk was smaller than that for 1d-2wk. Passive LV stiffness in infarcted LVs was higher than for non-infarcted LVs [249].

The tensile strength, strain at rupture, and stiffness of necrotic epicardium, mid-myocardium, endocardium, sub-epicardium, and visceral pericardium (VP) were measured based on isolated myocardial strips of the dog LVs at 24h after MI and compared with those of non-infarcted myocardium. Tensile strength of the endo- and epicardium was significantly higher than that of the mid-myocardium and sub-epicardium, but the VP was considerably stronger than any myocardium layer. Similar results were gained for stiffness. Strain at rupture was in a range of 0.40-0.53 and did not change from one layer to another. The higher the collagen content is, the stronger the strength at rupture is [250].

LV rupture threshold was studied by measuring the tensile strength of isolated infarcted myocardial strips, the force required to induce a tear in the central infarcted region, as shown in Fig. 11 and transmural pressure to rupture the infarcted LV after MI in rabbits. Late reperfusion (performed at 3h of MI) of transmural infarcts raised more resistance to infarct tearing and LV rupture in comparison with non-reperfused MI by 3d after MI [251]. Table 2 illustrates mean LV wall stress at rupture and LV wall tensile strength. Both thresholds are very similar to each other in values.

In the mouse model, rupture developed in LV free wall at 2-6d, and the measured rupture tension threshold was decreased to the minimum (40-60mN) at 3-4d from the maximum (110-120mN) at baseline/0d [252]. The reason for this is the most thinning wall at 3-4d as shown in Fig. 12.

5 Discussions

Myofibre and collagen fibre microstructures in MI zone are of vital importance in developing constitutive laws for infarcted myocardium. Indeed, there have been a number of experimental studies on this subject so far. Usually, MI is produced by blocking either LCX or LAD coronary artery. The MI created by this approach is obviously very similar to the actual MI in patients. However, MI has been created by using custom liquid-nitrogen-cooled cryoprobes as shown in [87], for example. The infarct caused from a cryoprobe might differ from the infarct due to coronary artery ligation at microstructure level of tissue. The scar tissue microstructures produced by different methods need to be compared at various MI ages in the same animal model in the future.

Uniaxial and biaxial tensile tests on passive infarct, border and remote tissues at various MI ages will form the basis for understanding of infarcted LV pumping function and development of constitutive law as well as its validation. Unfortunately, the experimental data of uniaxial and biaxial tensile tests on these tissues are lack, especially on large animal models and the human.

p-V curves in diastole are also necessary for validation of constitutive law for LV walls with MI. However, their experimental data for the human are very less presently. In [253], a combined pressure-conductance catheter is developed and can measure pressure and blood volume simultaneously in a LV positioned, thus pressure-time profiles in the LV chamber can be obtained in heart beating cycles. It is very hopeful that this catheter can find extensive applications in human LV chamber pressure and volume measurements in the future.

Active constitutive laws of LV myocardium with MI are equally important to quantitate impaired LV pumping function after MI. However, experiments on active myocardium with MI have drawn a little attention so far [211]. How the active contraction behaviour of myocardium with MI changes with time after MI is unclear presently.

There is a viscoelastic property in healthy and infarcted myocardium [227] in a 5min time scale, or a whole healthy LV in a 15min time scale, i.e. long-time scale [239]. In human cardiac cycle, the time scale (<1s) is too much shorter than those time scales used in the experiments, whether the viscoelastic property exists in myocardium in physiological heart beating time scale, i.e. short-time scale, needs to be identified in the future.

Very recently, intra-myocardial biomaterial injection therapy has become a promising technique for treating acute MI [254-256] and chronic heart failure [257]. How to in vivo characterise temporal changes in material properties of infarct region with injected substances during diastole is one of the key issues in assessment of the technique efficacy. An ultrasound [258-260] or MRI [261] and FEM-based approach proposed might be a feasible method for this purpose.

Nonetheless, new non-invasive techniques such as tissue tracking [262], Xstrain 4D [263] and CMR feature tracking [264] will add new content into biomechanics of infarcted myocardium in the very near future.

6 Conclusions

The experimental work in biomechanics of infarcted LVs has been reviewed at LV organ, tissue and microstructure levels. MI histology, LV remodelling process and mechanisms, temporal profiles of LV shape, volume, strain, regional function, *p*-*V* curves, pressure-length curves, passive stress-strain/stretch curves, LV rupture and viscoelasticity after MI have been shown and made clear. A few unsatisfactory research issues in experimental study on biomechanics of infarcted LVs have been argued and a couples of further research topics were suggested. Microstructure of infarcted cardiac tissue needs to be observed at microscale level intensively and to be correlated with passive biomechanical property by using updated constitutive laws. Active contraction experiments on infarcted myocardium are on demand to fully understand impaired LV pumping function and provide essential data for cardiac cycle modelling. Pressure-volume curves of LVs with MI in diastole and systole for the human are essential and desirable to validate new constitutive laws proposed for LV walls with MI.

Reference

[1] http://www.who.int/cardiovascular_diseases/priorities/secondary_prevention/country/en/index1.html.

[2] Bhatnagar P, Wickramasinghe K, Williams J, Rayner M and Townsend N, 2015, The epidemiology of cardiovascular disease in the UK 2014, Heart, 101(15), 1-8.

[3] Sutton M G and Shape N, 2000, Left ventricular remodelling after myocardial infarction, Circulation, 101(25), 2981-2988.

[4] Mallory K and White P D, The speed of healing of myocardial infarction, American Heart Journal, 1939, 18(6), 647-671

[5] Levine S A and Brown C L, 1929, Coronary thrombosis: its various clinical features, Medicine, 8(3), 245-418

[6] French B A and Kramer C M, 2007, Mechanisms of postinfarction left ventricle remodelling, Drug Discover Today: Disease Mechanisms, 4(3), 185-196.

[7] Karsner H T and Dwyer J E, 1916, Studies in infarction IV: Experimental bland infarction of the myocardium, myocardial regeneration and cicatrisation, Journal of Medical Research, 34(1), 21-39

[8] Lee L C, Kassab G S and Guccione J M, 2016, Mathematical modelling of cardiac growth and remodeling, WIREs System Biology and Medicine, 8, 211-226.

[9] Weisman H F and Healy B, 1987, Myocardial infarct expansion, infarct extension, and reinfarction: pathophysiologic diseases, Progress in Cardiovascular Diseases, 30(2), 73-110

[10] Sharpe N, 1992, Ventricular remodelling following myocardial infarction, American Journal of Cardiology, 70(10), 20-26

[11] Rumberger J A, 1994, Ventricular dilatation and remodeling after myocardial infarction, Mayo Clinic Proceedings, 69(7), 664-674

[12] Pfeffer M A, 1995, Left ventricular remodelling after acute myocardial infarction, Annual Review of Medicine, 46(10), 455-466

[13] Van de Werf F, Adrissino D, Betriu A, et al, 2003, Management of acute myocardial infarction in patients presenting with ST-segment elevation, European Heart Journal, 24, 28-66

[14] Jugdutt B I, 2003, Ventricular remodelling after infarction and the extracellular collagen matrix, Circulation, 108(11), 1395-1403

[15] Anderson J L and Morrow D A, 2017, Acute myocardial infarction, The New England Journal of Medicine, 376, 2053-2064

[16] Bhatt A S, Ambrosy A P and Velazquez E J, 2017, Adverse remodelling and reverse remodelling after myocardial infarction, Current Cardiology Reports, 19(8), 71. doi: 10.1007/s11886-017-0876-4

[17] Holmes J W, Borg T K and Covell J W, 2005, Structure and mechanics of healing myocardial infarcts, Annual Review of Biomedical Engineering, 7, 223-253

[18] Haywood L J, 1988, Treatment of myocardial infarction: a review, Journal of the National Medical Association, 80(4), 459-461

[19] Sun Y and Weber K T, 2000, Infarct scar: A dynamic tissue, Cardiovascular Research, 46(2), 250-256

[20] Topol E J, 2003, Current status and future prospects for acute myocardial infarction therapy, Circulation, 108(Supplement III), III-6- III-13

[21] Gorman R C, Jackson B M, Burdick J A, et al, 2011, Infarct restraint to limit adverse ventricular remodeling, Journal of Cardiovascular Translational Research, 4(1), 73-81

[22] Spath N B, Mills N L and Cruden N L, 2016, Novel cardioprotective and regenerative therapies in acute myocardial infarction: a review of recent and ongoing clinical trials, Future Cardiology, 12(6), 655-672

[23] Balotin N M, 1959, Myocardial infarction, its diagnosis and treatment: literature review, Chest, 36(1), 86-94

[24] Rozenman Y and Gotsman M S, 1994, The earliest diagnosis of acute myocardial infarction, Annals of Review Medicine, 45, 31-44

[25] Friedrich M G, 2008, Tissue characterization of acute myocardial infarction and myocarditis by cardiac magnetic resonance, Journal of American College of Cardiology-Cardiovascular Imaging, 1(5), 652-662

[26] Karamitsos T D, Dall'Armellina E, Choudhury R P, et al, 2011, Ischemic heart disease: comprehensive evaluation by cardiovascular magnetic resonance, American Heart Journal, 162(1), 16-30

[27] Ordovas K G and Higgins C B, 2011, Delayed contrast enhancement on MR Images of myocardium: past, present, future, Radiology, 261(2), 358-374

[28] Jiang K and Yu X, 2014, Quantification of regional myocardial wall motion by cardiovascular magnetic resonance, Quantitative Imaging in Medicine and Surgery, 4(5), 345-357

[29] D'Elia N, D'hooge J and Marwick T H, 2015, Association between myocardial mechanics and ischemic LV remodelling, Journal of American College Cardiology: Cardiovascular Imaging, 8(12), 1430-1433

[30] Mann D L, 1999, Mechanisms and models in heart failure-a combinatorial approach, Circulation, 100(9), 999-1008

[31] Jessup M and Brozena S, 2003, Heart failure, The New England Journal of Medicine, 348, 2007-2018

[32] Lewis A J, Burchell H B and Titus J L, 1969, Clinical and pathologic features of postinfarction cardiac rupture, American Journal of Cardiology, 23(1), 43-53

[33] Bates R J, Beutler S, Resnekov L, et al, 1977, Cardiac rupture-challenge in diagnosis and management, American Journal of Cardiology, 23(1), 43-53

[34] Solis C, Pujol D and Mauro V, 2009, Left ventricular free wall rupture after acute myocardial infarction, Revista Argentina de Cardiogla, 77(5), 1-9

[35] Venugopal J R, Prabhakaran P, Mukherjee S, et al, 2012, Biomaterial strategies for alleviation of myocardial infarction, Journal of the Royal Society Interface, 9, 1-19

[36] Gajarsa J J and Kloner R A, 2011, Left ventricular remodelling in the post-infarction heart: a review of cellular, molecular mechanisms, and therapeutic modalities, Heart Failure Review, 16(1), 13-21

[37] Bekkers S C A M, Yazdani S K and Virmani R, 2010, Microvascular obstruction, Journal of American College of Cardiology, 55(16), 1649-1660

[38] Vokonas P S, Malsky P M and Robbins S L, et al, 1978, Radioautographic studies in experimental myocardial infarction: profiles of ischemic blood flow and quantification of infarct size in relation to magnitude of ischemic zone, American Journal of Cardiology, 42(1), 67-75

[39] Kjekshus J K and Sobel B E, 1970, Depressed myocardial creatine phosphokinase activity following experimental myocardial infarction in rabbit, Circulation Research, 27(3), 403-414

[40] Hallen J, 2012, Troponin for the estimation of infarct size: what have we learned?, Cardiology, 121(3), 204-212

[41] Sobel B E, Bresnahan G F, Shell W E, et al, 1972, Estimation of infarct size in man and its relation to prognosis, Circulation, 46(4), 640-648

[42] Gibbons R J, 2011, Tc-99m SPECT sestamibi for the measurement of infarct size, Journal of Cardiovascular Pharmacology and Therapeutics, 16(3-4), 321-331

[43] Gibbons R J, Valeti U S, Araoz P A, et al, 2004, The quantification of infarct size, Journal of American College of Cardiology, 44(8), 1533-1542

[44] Pislaru S V, Ni Y, Pislaru C, et al, 1999, Noninvasive measurements of infarct size after thrombolysis with a necrosis-avid MRI contrast agent, Circulation, 99(5), 690-696

[45] Eichstaedt H W, Felix R, Danne O, et al, 1989, Imaging of acute myocardial infarction by magnetic resonance tomography (MRT) using the paramagnetic relaxation substance gadolinium-DTPA, Cardiovascular Drugs and Therapy, 3(5), 779-788

[46] Kim R J, Wu E, Rafael A, et al, 2000, The use of contrast-enhanced magnetic resonance imaging to identify reversible myocardial dysfunction, New England Journal of Medicine, 343(20), 1445-1453

[47] Fieno D S, Kim R J, Wu E, et al, 2000, Contrast-enhanced magnetic resonance imaging of myocardium at risk, Journal of American College of Cardiology, 36(6), 1985-1991

[48] Schuijf J D, Kaandorp T A M, Lamb H J, et al, 2004, Quantification of myocardial infarct size and transmurality by contrast-enhanced magnetic resonance imaging in men, American Journal of Cardiology, 94(3), 284-288

[49] Bulluck H, Dharmakumar R, Arai A E, et al, 2018, Cardiovascular magnetic resonance in acute ST-segment-elevation myocardial infarction, Circulation, 137(18), 1949-1964

[50] Petersen S E, Horstick G, Voigtlander T, et al, 2003, Diagnostic value of routine clinical parameters in acute myocardial infarction: a comparison to delayed contrast enhanced magnetic resonance imaging, International Journal of Cardiovascular Imaging, 19(5), 409-416

[51] Amado L C, Gerber B L, Gupta S N, et al, 2004, Accurate and objective infarct sizing by contrast-enhanced magnetic resonance imaging in a canine myocardial infarction model, Journal of American College Cardiology, 44(12), 2383-2389

[52] Kuhl H P, Papavasiliu T S, Beek A M, et al, 2004, Myocardial viability: rapid assessment with delayed contrast-enhanced MR imaging with three-dimensional inversion-recovery prepared pulse sequence, Radiology, 230(2), 576-582

[53] Hsu L Y, Natanzon A, Kellman P, et al, 2006, Quantitative myocardial infarction on delayed enhancement MRI. Part I: Animal validation of an automated feature analysis and combined thresholding infarct sizing algorithm, Journal of Magnetic Resonance Imaging, 23(3), 289-308

[54] Heiberg E, Ugander M, Engblom H, et al, 2008, Automated quantification of myocardial infarction from MR images by accounting for partial volume effects: Animal, phantom and human study, Radiology, 246(2), 581-588

[55] Kachenoura N, Rdheuil A, Herment A, et al, 2008, Robust assessment of the transmural extent of myocardial infarction in late gadolinium-enhanced MRI studies using appropriate angular and circumferential subdivision of the myocardium, European Radiology, 18(10), 2140-2147

[56] Peters D C, Appelbaum EA, Nezafat R, et al, 2009, Left ventricular infarct size, peri-infarct zone, and papillary scar measurements: A comparison of high-resolution 3D and conventional 2D late gadolinium-enhanced Cardiac MR, Journal of Magnetic Resonance Imaging, 30(4), 794-8007

[57] Neizel M, Katoh M, Schade E, et al, 2009, Rapid and accurate determination of relative infarct size in humans using contrast-enhanced magnetic resonance imaging, Clinical Research in Cardiology, 98(5), 319-324

[58] Mewton N, Revel D, Bonnefoy E, et al, 2011, Comparison of visual scoring and quantitative planimetry methods for estimation of global infarct size on delayed enhanced cardiac MRI and validation with myocardial enzymes, European Journal of Radiology, 78(1), 87-92

[59] Baron N, Kachenoura N, Cluzel P, et al, 2013, Comparison of various methods for quantitative evaluation of myocardial infarct volume from magnetic resonance delayed enhanced data, International Journal of Cardiology, 167(3), 739-744

[60] Vermes E, Childs H, Carbone I, et al, 2013, Auto-threshold quantification of left gadolinium enhancement in patients with acute heart disease, Journal of Magnetic Resonance Imaging, 37(2), 382-390

[61] Biere L, Mateus V, Grall S, et al, 2014, Late gadolinium enhancement MRI quantification to predict left ventricular remodeling after acute myocardial infarction, IRBM, 35(4), 182-188

[62] Karim R, Bhagirath P, Claus P, et al, 2016, Evaluation of state-of-the-art segmentation algorithm for left ventricle infarct from late gadolinium enhancement MR images, Medial Image Analysis, 30, 95-107

[63] Engblom H, Tufvesson J, Jablonowski R, et al, 2016, A new automatic algorithm for quantification of myocardial infarction imaged by late gadolinium enhancement cardiovascular magnetic resonance: experimental validation and comparison to expert delineations in multi-center, multi-vendor patient data, Journal of Cardiovascular Magnetic Resonance, 18, 27, doi.org/10.1186/s12968-016-0242-5

[64] Stillman A E, Odukerk M, Bluemke D, et al, 2011, Assessment of acute myocardial infarction: current status and recommendations from the North American society for cardiovascular imaging and the European society of cardiac radiology, International Journal Cardiovascular Imaging, 27(1), 7-24

[65] Pfeffer M A, Pfeffer J M, Fishbein M C, et al, 1979, Myocardial infarct size and ventricular function in rats, Circulation Research, 44(4), 503-512

[66] Schuster E H and Bulkley B H, 1979, Expansion of transmural myocardial infarction: a pathophysiologic factor in cardiac rupture, Circulation, 60(7), 1532-1538

[67] Warren S E, Royal H D, Markis J E, et al, 1988, Time course of left ventricular dilation after myocardial infarction: influence of infarct-related artery and success of coronary thrombolysis, Journal of American College of Cardiology, 11(1), 12-19

[68] Konermann M, Sanner B M, Horstmann E, et al, 1997, Changes of the left ventricle after myocardial infarction-estimation with cine magnetic resonance imaging during the first six month, Clinical Cardiology, 20, 201-212

[69] Christian T F, Behrenbeck T, Gersh B J, et al, 1991, Relation of left ventricular volume and function over one year after acute myocardial infarction to infarct size determined by technetium-99m sestamibi, American Journal of Cardiology, 68, 21-26

[70] Chareonthaitawee P, Christian T F, Hirose K, et al, 1995, Relation of initial size to extent of left ventricular remodelling in the year after acute myocardial infarction, American Journal of Cardiology, 25(3), 567-573

[71] Miller T D, Hodge D O, Sutton J M, et al, 1998, Usefulness of technetium-99m sestamibi infarct size in predicting posthospital mortality following acute myocardial infarction, American Journal of Cardiology, 81(12), 1491-1493

[72] Burns R J, Gibbons R J, Yi Q, et al, 2002, The relationships of left ventricular ejection fraction, end-systolic volume index and infarct size to six-month mortality after hospital discharge following myocardial infarction treated by thrombolysis, Journal of American College of Cardiology, 39(1), 30-36

[73] Roes S D, Kelle S, Kaandorp T A M, et al, 2007, Comparison of myocardial infarct size assessed with contrast-enhanced magnetic resonance imaging and left ventricular function and volumes to predict mortality in patients with healed myocardial infarction, American Journal of Cardiology, 100(6), 930-936

[74] Wu E, Ortiz J T, Tejedor P, et al, 2008, Infarct size by contrast enhanced cardiac magnetic resonance is a stronger predictor of outcomes than left ventricular ejection fraction or end-systolic volume index: prospective cohort study, Heart, 94(6), 730-736

[75] Kelle S, Roes S D, Klein C, et al, 2009, Prognostic value of myocardial infarct size and contractile reserve using magnetic resonance imaging, Journal of American College of Cardiology, 54(19), 1770-1777

[76] Bello D, Einhorn A, Kaushal R, et al, 2011, Cardiac magnetic resonance imaging: infarct size is an independent predictor of mortality in patients with coronary artery disease, Magnetic Resonance Imaging, 29(1), 50-56

[77] Sone G W, Selker H P, Thiele H, et al, 2016, Relationship between infarct size and outcomes following primary PCI, Journal of American College of Cardiology, 67(14), 1674-1683

[78] Ingkanison W P, Rhoads K L, Aletras A H, et al, 2004, Gadolinium delayed enhancement cardiovascular magnetic resonance correlates with clinical measures of myocardial infarction, Journal of American Collage Cardiology, 43(12), 2253-2259

[79] Pride Y B, Giuseffi J L, Mohanavelu S, et al, 2010, Relation between infarct size in ST-Segment elevation myocardial infarction treated successfully by percutaneous coronary intervention and left ventricular ejection fraction three months after the infarct, American Journal of Cardiology, 106(5), 635-640

[80] Grande P and Pedersen A, 1984, Myocardial infarct size: correlation with cardiac arrhythmias and sudden death, European Heart Journal, 5(8), 622-627

[81] Alegria J R, Miller T D, Gibbons R J, et al, 2007, Infarct size, ejection fraction, and mortality in diabetic patients with acute myocardial infarction treated with thrombolytic therapy, American Heart Journal, 154(4), 743-750

[82] Cannon R O, Butany J W, McManus B M, et al, 1983, Early degradation of collagen after acute myocardial infarction in the rat, American Journal of Cardiology, 52(3), 390-395

[83] Whittaker P, Boughner D R and Kloner R A, 1989, Analysis of healing after myocardial infarction using polarized light microscopy, American Journal of Pathology, 143(4), 879-893

[84] McCormick R J, Musch T I, Bergman B C, et al, 1994, Regional differences in LV collagen accumulation and mature cross-linking after myocardial infarction in rats, American Journal of Physiology-Heart and Circulation Physiology, 266(1), H354-H359

[85] Holmes J W, Nunez J A and Covell J W, 1997, Functional implication of myocardial scar structure, American Journal of Physiology-Heart and circulation Physiology, 272(5), H2123-H2230

[86] Zimmerman S D, Karlon W J, Holmes J W, et al, 2000, Structural and mechanical factors influencing infarct scar collagen organization, American Journal of Physiology-Heart and circulation Physiology, 278(1), H194-H200

[87] Fomovsky G M, Rouillard A D and Holmes J W, 2012, Regional mechanics determine collagen fiber structure in healing myocardial infarcts, Journal of Molecular and Cellular Cardiology, 52(5), 1083-1090

[88] Hervas A, Ruiz-Sauri A, de Dios E, 2016, Inhomogeneity of collagen organization within the fibrotic scar after myocardial infarction; results in a swine model and in human samples, Journal of Anatomy, 228(1), 47-58

[89] Chen J, Song S K, Liu W, et al, 2003, Remodeling of cardiac fiber structure after infarction in rats quantified with diffusion tensor MRI, American Journal of Physiology-Heart and circulation Physiology, 285(3), H1946-H954

[90] Wickline S A, Verdonk E D, Wong A K, et al, 1992, Structural remodelling of human myocardial tissue after infarction, Circulation, 85(1), 259-268

[91] Walker J C, Guccione J M, Jiang Y, et al, 2005, Helical myofiber orientation after myocardial infarction and left ventricular surgical restoration, Journal of Thoracic and cardiovascular Surgery, 129(2), 382-390

[92] Fomovsky G M and Holmes J W, 2010, Evolution of scar structure, mechanics, and ventricular function after myocardial infarction in the rat, American Journal of Physiology-Heart and Circulation Physiology, 298(1), H221-H228

[93] Zhou X, Yun J L, Han Z Q, et al, 2011, Postinfarction healing dynamics in the mechanically unloaded rat left ventricle, American Journal of Physiology-Heart and circulation Physiology, 300(5), H1863-H1874

[94] Kloner R A, Ganote C E and Jennings R B, 1974, The “no-reflow” phenomenon after temporary coronary occlusion in the dog, Journal of Clinical Investigation, 54(3), 1496-1508

[95] Wu K C, Kim R J, Bluemke D A, et al, 1998, Quantification and time course of microvascular obstruction by contrast-enhanced echocardiography and magnetic resonance imaging following acute myocardial infarction and reperfusion, Journal of American College of Cardiology, 32(6), 1756-1764

[96] Rochitte C E, Lima J A C, Bluemke D A, et al, 1998, Magnitude and time course of microvascular obstruction and tissue injury after acute myocardial infarction, Circulation, 98(10), 1006-1014

[97] Wu K C, Zerhouni E A, Judd R M, et al, 1998, Prognostic significance of microvascular obstruction by magnetic resonance imaging in patients with acute myocardial infarction, Circulation Research, 97(8), 765-772

[98] Gerber B L, Rochitte C E, Lima J A C, et al, 2000, Microvascular obstruction and left ventricular remodelling early after acute myocardial infarction, Circulation, 101(23), 2734-2741

[99] Choi C J, Haji-Momenian S, DiMaria J M, et al, 2004, Infarct involution and improved function during healing of acute myocardial infarction: the role of microvascular obstruction, Journal of Cardiovascular Magnetic Resonance, 6(4), 917-925

[100] Bogaert J, Kalantzi M, Rademakers F E, et al, 2007, Determinants and impact of microvascular obstruction in successfully reperfused ST-segment elevation myocardial infarction: assessment by magnetic resonance imaging, European Radiology, 17(10), 2572-2580

[101] Everaars H, Robbers L F H J, Gotte M, et al, 2018, Strain analysis is superior to wall thickening in discriminating between infarcted myocardium with and without microvascular obstruction, European Radiology, 28(12), 5171-5181

[102] Hutchins G M and Bulkley B H, 1978, Infarct expansion versus extension: two different complications of acute myocardial infarction, American Journal of Cardiology, 41(7), 1127-1132

[103] Eaton L W and Bulkley B H, 1981, Expansion of acute myocardial infarction: its relationship to infarct morphology in a canine model, Circulation Research, 49(1), 80-88

[104] Hochman J S and Bulkley B H, 1982, Expansion of acute myocardial infarction: an experimental study, Circulation, 65(7), 1446-1450

[105] Roberts C S, MaClean D, Maroko P, et al, 1984, Early and late remodelling of the left ventricle after acute myocardial infarction, American Journal of Cardiology, 54(3), 407-410

[106] Jugdutt B I and Amy R W, 1986, Healing after myocardial infarction in the dog: changes in infarct hydroxproline and topography, Journal of American College of Cardiology, 7(1), 91-102

[107] Kass D A, Maughan W L, Ciuffo A, et al, 1988, Disproportionate epicardial dilation after transmural infarction of the canine left ventricle: acute and chronic differences, Journal of American College of Cardiology, 11(1), 177-185

[108] Gaudron P, Eilles C, Ertl G, et al, 1990, Early remodelling of the left ventricle in patients with myocardial infarction, European Heart Journal, 11(Supplement B), 139-146

[109] Gaudron P, Eilles C, Ertl G, et al, 1992, Compensatory and noncompensatory left ventricular dilatation after myocardial infarction: time course and hemodynamic consequences at rest and during exercise, American Heart Journal, 123(2), 377-3385

[110] Gaudron P, Eilles C, Kugler I, et al, 1993, Progressive left ventricular dysfunction and remodelling after myocardial infarction, Circulation, 87(3), 755-763

[111] Pokormey S D, Rodrigues J, Ortiz J T, et al, 2012, Infarct healing is a dynamic process following acute myocardial infarction, Journal of Cardiovascular Magnetic Resonance, 14: 62. doi: 10.1186/1532-429X-14-62

[112] McKay R G, Pfeffer M A, Pasternak R C, et al, 1986, Left ventricular remodelling after myocardial infarction: a corollary to infarct expansion, Circulation, 74(4), 693-702

[113] Grossman W, Jones D and McLaurin L P, 1975, Wall stress and patterns of hypertrophy in the human left ventricle, Journal of Clinical Investigation, 56(1), 56-64

[114] Grossman W, 1980, Cardiac hypertrophy: useful adaptation or pathologic process ?, American Journal of Medicine, 69(4), 56-64

[115] Spotnitz H M, Spotnitz W D, Cottrell T S, et al, 1974, Cellular basis for volume related wall thickness changes in the rat left ventricle, Journal of Molecular and Cellular Cardiology, 6(4), 317-331

[116] Crozatier E, Ashraf M, Franklin D, et al, 1977, Sarcomere length in experimental myocardial infarction: evidence for sarcomere overstretch in dyskinetic ventricular regions, Journal of Molecular and Cellular Cardiology, 9(10), 785-797

[117] Weisman H F, Bush D E, Mannisi J A, et al, 1988, Cellular mechanisms of myocardial infarct expansion, Circulation, 78(1), 186-201

[118] Olivetti G, Capasso J M, Sonnenblick E H, et al, 1990, Side-to-side slippage of myocytes participates in ventricular wall remodelling acutely after myocardial infarction in rats, Circulation Research, 67(1), 23-34

[119] Olivetti G, Capasso J M, Meggs L G, et al, 1991, Cellular basis of chronic ventricular remodelling after myocardial infarction in rats, Circulation Research, 68(3), 856-969

[120] Anversa P, Olivetti G and Capasso J M, 1991, Cellular basis of ventricular remodelling after myocardial infarction, American Journal of Cardiology, 68(14), 7-16

[121] Whittaker P, Boughner D R, Kloner R A, 1991, Role of collagen in acute myocardial infarct expansion, Circulation, 84(5), 2123-2134

[122] Kramer C M, Rogers W J, Park C S, et al, 1998, Regional myocyte hypertrophy parallels regional myocardial dysfunction during post-infarct remodelling, Journal of Molecular and Cell Cardiology, 30(9), 1773-1778

[123] Sam F, Sawyer D B, Chang D L F, et al, 2000, Progressive left ventricular remodelling and apoptosis late after myocardial infarction in mouse heart, American Journal of Physiology-Heart and Circulation Physiology, 279(1), H422-H428

[124] Zimmerman S D, Criscione J B and Covell J W, 2004, Remodeling in myocardium adjacent to an infarction in the pig left ventricle, American Journal of Physiology-Heart and Circulation Physiology, 287(6), H2697-H2704

[125] Rogers W J, Hood W P, Mantle J A, et al, 1984, Return of left ventricular function after reperfusion in patients with myocardial infarction: importance of subtotal stenosis or infarct collaterals, Circulation, 69(2), 338-349

[126] Jugdutt B I, 1985, Delayed effect of early infarct-limiting therapies on healing after myocardial infarction, Circulation, 72(4), 907-914

[127] Pfeffer M A and Brauneald E, 1990, Ventricular remodeling after acute myocardial infarction, Circulation, 81(4), 1161-1172

[128] Litwin S E, Litwin C M, Raya T E, et al, 1991, Contractility and stiffness of noninfarcted myocardium after coronary ligation in rats, Circulation, 83(3), 1028-1037

[129] Brauneald E and Pfeffer M A, 1991, Ventricular enlargement and remodeling following acute myocardial infarction: mechanisms and management, American Journal of Cardiology, 68(1), 1-6

[130] Kumar R, Sharma G V R K, Molokhia F A, et al, 1972, Experimental myocardial infarction X. efficacy of glucagon in acute and healing phase in intact conscious dogs: effects on hemodynamics and myocardial oxygen consumption, Circulation, 45(1), 55-64

[131] Hseh P C H, Davis M E, Gannon J, et al, 2006, Controlled delivery of PDGF-BB for myocardial protection using injectable self-assembling peptide nanofibers, Journal of Clinical Investigation, 116(1), 237-248

[132] Leor J, Tuvia S, Guetta V, et al, 2009, Intracoronary injection of in situ forming alginate hydrogel reverses left ventricular remodelling after myocardial infarction in swine, Journal of American College of Cardiology, 54(11), 1014-1022

[133] Yu J, Christman K L and Chin E, 2009, Restoration of left ventricular geometry and improvement of left ventricular function in a rodent model of chronic ischemic cardiomyopathy, Journal of Thoracic and cardiovascular Surgery, 137(1), 180-186

[134] Ryan LP, Matsuzaki K, Noma M, et al, 2009, Dermal filler injection: a novel approach for limiting infarct expansion, Annals of Thoracic Surgery, 87(1), 148-156

[135] Ifkovits J L, Tous E, Minakawa M, et al, 2010, Injectable hydrogel properties influence infarct expansion and extent of postinfarction left ventricular remodelling in an ovine model, PNAS, 107(25), 11507-11512

[136] Morita M, Eckert C E, Matszaki K, et al, 2011, Modification of infarct material properties limits adverse ventricular remodelling, Annals of Thoracic Surgery, 92(2), 617-625

[137] Wenk F F, Eslami P, Zhang Z, et al, 2011, A novel method for quantifying the in-vivo mechanical effect of material injected into a myocardial infarction, Annals of Thoracic Surgery, 92(3), 935-941

[138] Dorsey S M, McGarvey J R, Wang H, et al, 2015, MRI evaluation of injectable hyaluronic acid-based hydrogel therapy to limit ventricular remodelling after myocardial infarction, Biomaterials, 69, 65-75

[139] Zhu Y, Wood N A, Fok K, et al, 2016, Design of a coupled thermoresponsive hydrogel and robotic system for postinfarct biomaterial injection therapy, Annals of Thoracic Surgery, 102(3), 780-786

[140] Dai W, Wold L E, Dow J S, et al, 2005, Thickening of the infarcted wall by collagen injection improves left ventricular function in rats, Journal of American College of Cardiology, 46(4), 714-719

[141] Chung E S, Dan D, Solomon S D, et al, 2010, Effect of peri-infarct pacing early after myocardial infarction, Circulation-Heart Failure, 3(6), 650-658

[142] Klepach D, Lee L C, Wenk J F, et al, 2012, Growth and remodelling of the left ventricle: a case study of myocardial infarction and surgical ventricular restoration, Mechanics Research Communications, 42, 134-141

[143] Pilla J J, Blom A S and Brockman D J, 2003, Passive ventricular constraint to improve left ventricular function and mechanics in an ovine model of heart failure secondary to acute myocardial infarction, Journal of Thoracic and Cardiovascular Surgery, 126(5), 1467-1475

[144] Kass D A, Traill T A, Keating M, et al, 1988, Abnormalities of dynamic ventricular shape change in patients with aortic and mitral valvular regurgitation: assessment by Fourier shape analysis and global geometric indexes, Circulation Research, 62(1), 127-138

[145] Weisman H F, Bush D E, Mannisi J A, et al, 1985, Global cardiac remodelling after acute myocardial infarction: a study in the rat model, Journal of American College of Cardiology, 5(6), 1355-1362

[146] Bau L H B, Schipperheyn J J, van der Wall E E, et al, 1996, Regional myocardial shape alterations in patients with anterior myocardial infarction, International Journal of Cardiac Imaging, 12(2), 89-96

[147] Capasso J M, Li P, Zhang X, et al, 1992, Heterogeneity of ventricular remodeling after acute myocardial infarction in rats, American Journal of Physiology-Heart and Circulation Physiology, 262(2), H486-H495

[148] Bogaert J, Bosmans H, Maes A, et al, 2000, Remote myocardial dysfunction after acute anterior myocardial infarction: impact function of left ventricular shape on regional, Journal of American College of Cardiology, 35(6), 1525-1534

[149] Wong S P, French J K, Lydon A M, et al, 2004, Relation of left ventricular sphericity to 10-year survival after acute myocardial infarction, American Journal of cardiology, 94(15), 1270-1275

[150] Di Donato M, Dabic P, Castelvecchio S, et al, 2006, Left ventricular geometry in normal and post-anterior myocardial infarction patients: sphericity index and 'new' conicity index comparisons, European Journal of Cardio-Thoracic Surgery, 29(Supplement 1), S225-S230

[151] Fan H, Zheng Z, Feng W, et al, 2010, Apical conicity ratio: a new index on left ventricular apical geometry after myocardial infarction, Journal of Thoracic and Cardiovascular Surgery, 140(6), 1402-1407

[152] Calafiore A M, Iaco A L, Amata D, et al, 2010, Left ventricular surgical restoration for anteroseptal scars: volume versus shape, Journal of Thoracic and Cardiovascular Surgery, 139(5), 1123-1130

[153] Di Mauro M, Iaco A L, Bencivenga S, et al, 2015, Left ventricular surgical remodelling: is it a matter of shape or volume, European Journal of Cardio-Thoracic Surgery, 47(3), 473-479

[154] Ardekani S, Weiss R G, Lardo A C, et al, 2009, Computational method for identifying and quantifying shape features of human left ventricular remodelling, Annals of Biomedical Engineering, 37(6), 1043-1054

[155] Zhang X, Cowan B R, Bluemke D A, et al, 2014, Atlas-based quantification of cardiac remodelling due to myocardial infarction, PLoS One, 9(10), e110243

[156] Lessick J, Sideman S, Azhari H, et al, 1991, Regional three-dimensional geometry and function of left ventricles with fibrous aneurysms, Circulation, 84(3), 1072-1086

[157] Jackson B M, Gorman III J H, Salgo I S, et al, 2002, Border zone geometry increases wall stress after myocardial infarction: contrast echocardiographic assessment, American Journal of Physiology-Heart and Circulation Physiology, 284, H475-H479

[158] Jackson B M, Parish L M, Gorman III J H, et al, 2005, Border zone geometry after acute myocardial infarction: a three-dimensional contrast enhanced echocardiographic study, Annals of Thoracic Surgery, 80(6), 2250-2256

[159] Waris E K, Siitonen L and Himanka E, 1966, Heart size and prognosis in myocardial infarction, American Heart Journal, 71(2), 187-195

[160] Hood W B, McCarthy B and Lown B, 1967, Myocardial infarction following coronary ligation in dogs, Circulation Research, 21(2), 191-199

[161] Kostuk W J, Kazamias T M, Gander M P, et al, 1973, Left ventricular size after acute myocardial infarction, Circulation, 47(6), 1174-1179

[162] Weisse A B, Saffa R S, Levinson G E, et al, 1970, Left ventricular function during the early and late stages of scar formation following experimental myocardial infarction, American Heart Journal, 79(3), 370-383

[163] Field B J, Russell R O, Moraski R E, et al, 1974, Left ventricular size and function and heart size in the rear following myocardial infarction, Circulation, 50(2), 331-339

[164] White H D, Noris R M, Brown M A, et al, 1987, Left ventricular end-systolic volume as the major determinant of survival after recovery from myocardial infarction, Circulation, 76(1), 44-51

[165] Gadsboll N, Hoilund-Carlsen P H, Badsberg J H, et al, 1989, Late ventricular dilatation survivors of acute myocardial infarction, American Journal of Cardiology, 64(16), 961-966

[166] Mitchell G F, Lamas G A, Vaughan D E, et al, 1992, Left ventricular remodeling in the year after first anterior myocardial infarction: a quantitative analysis of contractile segment length and ventricular shape, Journal of American College of Cardiology, 19(6), 1136-1144

[167] Sutton M J, Pfeffer M A and Plappert T, 1994, Quantitative two-dimensional echocardiographic measurements are major predictor of adverse cardiovascular events after acute myocardial infarction, Circulation, 89(1), 68-75

[168] Nicolosi G K, Voors A A, et al, 2002, Prediction of 6 months left ventricular dilatation after myocardial infarction in relation to cardiac morbidity and mortality, European Heart Journal, 23(7), 536-542

[169] Mielniczuk L M, Lamas G A, Flaker G C, et al, 2007, Left ventricular end-diastolic pressure and risk of subsequent heart failure in patients following an acute myocardial infarction, Congest Heart Failure, 13(4), 209-214

[170] O'Regan D P, Shi W, Aiff B, et al, 2012, Remodeling after acute myocardial infarction: mapping ventricular dilatation using three dimensional CMR image registration, Journal of Cardiovascular Magnetic Resonance, 14, 41, doi: 10.1186/1532-429X-14-41

[171] Protti A, Dong X, Sirker A, et al, 2012, MRI-based prediction of adverse cardiac remodelling after murine myocardial infarction, American Journal of Physiology-Heart and Circulation Physiology, 303(3), H309-H314

[172] Bulluck H, Go Y Y, Crimi G, et al, 2017, Defining left ventricular remodelling following acute ST-segment elevation myocardial infarction using cardiovascular magnetic resonance, Journal of Cardiovascular Magnetic Resonance, 19, 26, doi.org/10.1186/s12968-017-0343-9

[173] Field B J, Russell R O, Dowling J T, et al, 1972, Regional left ventricular performance in the year following myocardial infarction, Circulation, 46(4), 679-689

[174] Theroux P, Franklin D, Ross J, et al, 1974, Regional myocardial function during acute coronary artery occlusion and its modification by pharmacologic agents in the dog, Circulation Research, 35(6), 896-908

[175] Lew W Y W, Chen Z, Guth B, et al, 1985, Mechanisms of augmented segment shortening in nonischaemic areas during acute ischemia of the canine left ventricle, Circulation Research, 56(3), 351-358

[176] Theroux P, Ross J and Franklin D, 1977, Regional myocardial function and dimensions early and late after myocardial infarction in the unanesthetized dog, Circulation Research, 40(2), 158-165

[177] Kramer C M, Lima J A C, Reichek N, et al, 1993, Regional differences in function within noninfarcted myocardium during left ventricular remodelling, Circulation, 88(3), 1279-1288

[178] Gallagher K P, Gerren R A, Stirling M C, et al, 1986, The distribution of function impairment across the lateral border of acutely ischemic myocardium, Circulation Research, 58(4), 570-583

[179] Chan W, Duffy S J, White D A, et al, 2012, Acute left ventricular remodelling following myocardial infarction, Journal of American Collage Cardiology-Cardiovascular Imaging, 5(9), 884-893

[180] Omens J H, Miller T R, Covell J W, 1997, Relationship between passive tissue strain and collagen uncoiling during healing of infarcted myocardium, Cardiovascular Research, 33(2), 351-358

[181] Young A A, French B A, Yang Z, et al, 2006, Reperfused myocardial infarction in mice: 3D mapping of late gadolinium enhancement and strain, Journal of Cardiovascular Magnetic Resonance, 8(5), 685-692

[182] Lima J A C, Ferrari V A, Reichek N, et al, 1995, Segmental motion and deformation of transmurally infarcted myocardium in acute postinfarct period, American Journal of Physiology-Heart and Circulation Physiology, 268, H1304-H1312

[183[Mazhari R, Omens J H, Covell J W, et al, 2000, Structural basis of regional dysfunction in acutely ischemic myocardium, Cardiovascular Research, 47(2), 284-293

[184] Pilla J J, Koomalsingh K J, McGarvey J R, et al, 2015, Regional myocardial three-dimensional principal strains during postinfarction remodelling, Annals of Thoracic Surgery, 99, 770-778

[185] Hung C L, Verma A, Uno H, et al, 2010, Longitudinal and circumferential strain rate, left ventricular remodelling, and prognosis after myocardial infarction, Journal of American Collage Cardiology, 56(22), 1812-1822

[186] Omens J H and Covell J W, 1991, Transmural distribution of myocardial tissue growth induced by volume-overload hypertrophy, Circulation, 84(3), 1235-1245

[187] Holmes J W, Yamashita H, Waldman L K, et al, 1994, Scar remodeling and transmural deformation after infarction in the pig, Circulation, 90(1), 411-420

[188] Tsamis A, Cheng A, Nguyen T C, et al, 2012, Kinematics of cardiac growth: in vivo characterization of growth tensors and strains, Journal of the Mechanical Behavior of Biomedical Materials, 8, 165-177

[189] Huttin O, Coiro S, Selton-Suty C, et al, 2016, Prediction of left ventricular remodeling after a myocardial infarction: role of myocardial deformation: a systematic review and meta-analysis, PLoS ONE 11(12): e0168349. doi:10.1371/journal. pone.0168349

[190] Hill A V, 1938, The heat of shorting and the dynamic constants of muscle, Proceedings of Royal Society, Series B, 126, 136-195

[191] Sonnenblick E H, 1961, Force-velocity relations in mammalian heart muscle, American Journal of Physiology, 202(5), 931-939

[192] Sonnenblick E H, 1965, Instantaneous force-velocity-length determinants in the contraction of heart muscle, Circulation Research, 16(5), 441-451

[193] Noble M I, Bowen T E and Hefner L L, 1969, Force-velocity relationship of cat cardiac muscle, studied by isotonic and quick-release techniques, Circulation Research, 24(6), 821-833

[194] Forman R, Ford L E and Sonnenblick E H, 1972, Effect of muscle length on the force-velocity relationship of tetanized cardiac muscle, Circulation Research, 31(2), 195-206

[195] Edman K A P and Nilsson E, 1972, Relationships between force and velocity of shortening in rabbit papillary muscle, Acta physiologica Scandinavica, 85, 488-500

[196] Fry D L, Griggs D M and Greenfield J C, 1964, Myocardial mechanics: relationships of heart muscle, Circulation Research, 18(6), 729-744

[197] Levine H J and Britman N A, 1964, Force-velocity relations in the intact dog heart, Journal of Clinical Investigation, 43(7), 1383-1396

[198] Levine H, Forwand S A, McIntyre K M, et al, 1966, Effect of afterload on force-velocity relations and contractile element work in the intact heart, Circulation Research, 18(6), 729-744

[199] Covell J W, Ross J, Sonnenblick E H, et al, 1966, Comparison of the force-velocity relation and the ventricular function curve as measures of the contractile state of the intact heart, Circulation Research, 19(2), 364-372

[200] Taylor R R, Ross J, Covell J W, et al, 1967, A quantitative analysis of left ventricular myocardial function in the intact, sedated dog, Circulation Research, 21(2), 99-115

[201] Burns J W, Covell J W and Ross J, 1973, Mechanics of isotonic left ventricular contractions, American Journal of Physiology, 224(4), 725-732

[202] Ross J, Covell J W and Sonnenblick E H, 1967, The mechanics of left ventricular contraction in acute experimental cardiac failure, Journal of Clinical Investigation, 46(3), 299-312

[203] Mason D T, Spann J F and Zelis R, 1970, Quantification of the contractile state of the intact human heart, American Journal of Cardiology, 26(3), 248-257

[204] Sonnenblick E H, 1964, Series elastic and contractile elements in heart muscle: changes in muscle length, American Journal of Physiology, 207(6), 1330-1338

[205] Parmley W W, Spann J F, Taylor R R, et al, 1968, The series elasticity of cardiac muscle in hyperthyroidism, ventricular hypertrophy, and heart failure, Proceedings of Society for Experimental Biology and Medicine, 127(2), 606–609.

[206] Hugenholtz P G, Ellison C, Urschel C W, et al, 1970, Myocardial force-velocity relationships in clinical heart disease, Circulation, 41(2), 191-202

[207] Enright L P, Hannah III H and Reis R L, 1970, Effects of acute regional myocardial ischemia on left ventricular function in dogs, Circulation Research, 26(3), 307-315

[208] Little W C and O'Rourke R A, 1985, Effect of regional ischemia on the left ventricular end-systolic pressure-volume relation in chronically instrumented dogs, Journal of American College of Cardiology, 5(2), 297-302

[209] Matsuwaka R, Matuda H, Shirakura R, et al, 1994, Changes in left ventricular performance after global ischemia: assessing LV pressure-volume relationship, Annals of Thoracic Surgery, 57(1), 151-156

[210] Little W C, Park R C and Freeman G L, 1987, Effects of regional ischemia and ventricular pacing on LV dp/dt_{max}-end-diastolic volume relation, American Journal of Physiology-Heart and Circulation Physiology, 252, H933-H940

[211] Forwand S A, McIntyre K M, Lipana J G, et al, 1966, Active stiffness of the intact canine left ventricle, Circulation Research, 19(4), 970-979

[212] Kumar R, Hood W B, Joison J, et al, 1970, Experimental myocardial infarction: II acute depression and subsequent recovery of left ventricular function: serial measurements in intact conscious dogs, Journal of Clinical Investigation, 49(1), 55-62

[213] Hood W B, Bianco J A, Kumar R, et al, 1970, Experimental myocardial infarction: IV reduction of left ventricular compliance in the healing phase, Journal of Clinical Investigation, 49(7), 1316-1323

[214] Forrester J S, Diamond G, Parmley W W, et al, 1972, Early increase in left ventricular compliance after myocardial infarction, Journal of Clinical Investigation, 51(3), 598-603

[215] Fletcher P J, Pfeffer J M and Pfeffer M A, 1981, Left ventricular diastolic pressure-volume relations in rats with healed myocardial infarction, Circulation Research, 49(3), 618-626

[216] Mathey D, Bleifeld W and Franken G, 1974, Left ventricular relaxation and diastolic stiffness in experimental myocardial infarction, Cardiovascular Research, 8(5), 583-592

[217] Diamond G and Forrester J S, 1972, Effect of coronary artery disease and acute myocardial infarction on left ventricular compliance in man, Circulation, 45(1), 11-19

[218] Raya T E, Gay R G, Lancaster L, et al, 1988, Serial changes in left ventricular relaxation and chamber stiffness after larger myocardial infarction in rats, Circulation, 77(6), 1424-1431

[219] Wu H, Li L, Niu O, et al, 2017, The structure-function remodeling in rabbit hearts of myocardial infarction, Physiological Reports, 5(12), 1-13

[220] Tyberg J V, Forrester J S, Wyatt H L, et al, 1974, An analysis of segmental ischemic dysfunction utilizing the pressure-length loop, Circulation, 49(4), 748-754

[221] Vokonas P S, Pirzada F A and Hood W B, 1976, Experimental myocardial infarction XII: dynamic changes in segmental mechanical behaviour of infarcted and non-infarcted myocardium, American Journal of Cardiology, 37(6), 853-859

[222] Pirzada F A, Ekong E A, Vokonas P S, 1976, Experimental myocardial infarction XIII: sequential changes in left ventricular pressure-length relationships in the acute phase, Circulation, 53(6), 970-975

[223] Akaishi M, Weintraub W S, Schneider R M, et al, 1986, Analysis of systolic bulging, Circulation Research, 58(2), 209-217

[224] Laird J D and Vellekoop H P, 1977, Time course of passive elasticity of myocardial tissue following experimental infarction in rabbits and its relation to mechanical dysfunction, Circulation Research, 41(5), 715-721

[225] Fung Y C, 1967, Elasticity of soft tissues in simple elongation, American Journal of Physiology, 213, 1532-1544

[226] Connelly C M, McLaughlin R J, Vogel W M, et al, 1991, Reversible and irreversible elongation of ischemic, infarcted, and healed myocardium in response to increases in preload and afterload, Circulation, 84(1), 387-399

[227] Gupta K B, Ratcliffe M B, Fallert M A, et al, 1994, Changes in passive mechanical stiffness of myocardial tissue with aneurysm formation, Circulation, 89(5), 2315-2326

[228] Lundin G, 1946, The influence of g-strophantin on the mechanical properties of cardiac muscle, Acta physiologica Scandinavica, 11(2-3), 221-229

[229] Hoffman B F, Bassett A L and Bartelstone H J, 1968, Some mechanical properties of isolated mammalian cardiac muscle, Circulation Research, 23(2), 291-311

[230] Little R C and Wead W B, 1971, Diastolic viscoelastic properties of active and quiescent cardiac muscle, American Journal of Physiology, 221(4), 1120-1125

[231] Pinto J G and Fung Y C, 1973, Mechanical properties of the heart muscle in the passive state, Journal of Biomechanics, 6(6), 597-616

[232] Noble M I M, 1977, The diastolic viscous properties of cat papillary muscle, Circulation Research, 40(3), 288-292

[233] Loeffler L and Sagawa K, 1975, A one-dimensional viscoelastic model of cat heart muscle studied by small length perturbations during isometric contraction, Circulation Research, 36(4), 498-512

[234] Chiu Y L, Ballou E W and Ford L E, 1982, Internal viscoelastic loading in cat papillary muscle, Biophysical Journal, 40(2), 109-120

[235] Hefner L L, Coghlan H C, Jones W B, et al, 1961, Distensibility of the dog left ventricle, American Journal Physiology, 201(1), 97-101

[236] Noble M I M, Milne E N C, Goerke R J, et al, 1969, Left ventricular filling and diastolic pressure-volume relations in the conscious dog, Circulation Research, 24(2), 269-283

[237] Templeton G H, Ecker R R and Mitchell J H, 1972, Left ventricular stiffness during diastole and systole: the influence of changed in volume and inotropic state, Cardiovascular Research, 6(1), 95-100

[238] Horwitz L D and Bishop V S, 1972, Left ventricular pressure-dimension relationships in the conscious dog, Cardiovascular Research, 6(2), 163-171

[239] Rankin J S, Arentzen C E, McHale P A, et al, 1977, Viscoelastic properties of the diastolic left ventricle in the conscious dog, Circulation Research, 41(1), 37-45

[240] Pouleur H, Karliner J S, LeWinter M M, et al, 1979, Diastolic viscous properties of the intact canine left ventricle, Circulation Research, 45(3), 410-419

[241] Hess O M, Grimm J and Krayenbuehl H P, 1979, Diastolic simple elastic and viscoelastic properties of the left ventricle in man, Circulation Research, 59(6), 1178-1187

[242] Hess O M, Schneider J, Koch R, et al, 1981, Diastolic function and myocardial structure in patients with myocardial hypertrophy, Circulation, 63(2), 360-371

[243] Hess O M, Osakada G, Lavelle J F, et al, 1983, Diastolic myocardial wall stiffness and ventricular relaxation during partial and complete coronary occlusion in the conscious dog, Circulation Research, 52(4), 387-400

[244] Visner M S, Arentzen C E, Parrish D G, et al, 1985, Effects of global ischemia on the diastolic properties of the left ventricular in the conscious dog, Circulation, 71(3), 610-619

[245] Connelly C M, Vogel W M, Wiegner A W, et al, 1985, Effects of reperfusion after coronary artery occlusion on post-infarction scar tissue, Circulation Research, 57(4), 562-577

[246] Kendall R W and DeWood M A, 1978, Postinfarction cardiac rupture: surgical success and review of the literature, Annals of Thoracic Surgery, 25(4), 311-315

[247] Mann J M and Roberts W C, 1988, Rupture of the left ventricular free wall during acute myocardial infarction: analysis of 138 necropsy patients and comparison with 50 necropsy patients with acute myocardial infarction without rupture, American Journal of Cardiology, 62(13), 847-859

[248] Lerman R H, Apstein C S, Kagan H M, et al, 1983, Myocardial healing and repair after experimental infarction in the rabbit, Circulation Research, 53(3), 378-388

[249] Jugdutt B I, 1987, Left ventricular rupture threshold during the healing phase after myocardial infarction in the dog, Canadian Journal of Physiology, 65(3), 307-316

[250] Przyklenk K, Connelly C M, McLaughlin R J, et al, 1987, Effect of myocyte necrosis on strength, strain, and stiffness of isolated myocardial strips, American Heart Journal, 114(6), 1349-1359

[251] Connelly C M, Ngoy S, Schoen F J, et al, 1992, Biomechanical properties of reperfused transmural myocardial infarcts in rabbits during the first week after infarction, Circulation Research, 71(2), 401-413

[252] Gao X M, Xu Q, Kiriazis H, et al, 2005, Mouse model of post-infarct ventricular rupture; time course, strain- and gender-dependency, tensile strength, and histopathology, Cardiovascular Research, 65(2), 5469-477

[253] Steendijk P, Tulner S A F, Wiemer M, et al, 2004, Pressure-volume measurements by conductance catheter during cardiac resynchronization therapy, European heart Journal Supplements, 6(Supplement D), D35-D42

[254] Nelson D M, Ma Z, Fujimoto K L, et al, 2011, Intra-myocardial biomaterial injection therapy in the treatment of heart failure: Materials, outcomes and challenges, Acta Biomaterialia, 7, 1-15

[255] Yoshizumi T, Zhu Y, Jiang H, et al, 2016, Timing effect of intramyocardial hydrogel injection for positively impacting left ventricular remodeling after myocardial infarction, Biomaterials, 83, 182-193

[256] Zhu Y, Matsumura Y and Wagner W R, 2017, Ventricular wall biomaterial injection therapy after myocardial infarction: advances in material design, mechanistic insight and early clinical experiences, Biomaterials, 129, 37-53

[257] Sabbah H N, Wang M, Gupta R C, et al, 2013, Augmentation of left ventricular wall thickness with alginate hydrogel implants improves left ventricular function and prevents progressive remodeling in dogs with chronic heart failure, Journal of American College of Cardiology-Heart Failure, 1(3), 253-257

[258] Fan L, Yao J, Yang C, et al, Infarcted left ventricles have stiffer material properties and lower stiffness variation: 3D echo-based modeling to quantify in vivo ventricle material properties, ASME Journal of Biomechanical Engineering, 2015, 137(8), 081005

[259] Fan L, Yao J, Yang C, et al, Material stiffness parameters as potential predictors of presence of left ventricle myocardial infarction: 3D echo-based computational modeling study, Biomedical Engineering Online, 2016, 15:34, doi:10.1186/s12938-016-0151-8

[260] Fan L, Yao J, Yang C, et al, Modeling active contraction and relaxation of left ventricle using different zero-load diastole and systole geometries for better material parameter estimation and stress/strain calculations, Molecular & Cellular Biomechanics, 2016, 13(1), 44-68

[261] McGarvey J R, Mojssejenko D, Shauna M S, et al, 2015, Temporal changes in infarct material properties: an in vitro assessment using magnetic resonance imaging and finite element simulations, Annals of Thoracic Surgery, 100(2), 582-590

[262] Claus P, Omar A M S, Pedrzzetti G, et al, 2015, Tissue tracking technology for assessing cardiac mechanics, Journal of American College of Cardiology-Cardiovascular Imaging, 8(32), 1444-1460

[263] D'Andrea A, Mele D, Agricola E, et al, 2016, XStrain 4D analysis predicts left ventricular remodelling in patients with recent non-ST-segment elevation myocardial infarction, International Journal of Cardiology, 206, 107-109

[264] Feisst A, Kuetting D L R, Dabir D, et al, 2018, Influence of observer experience on cardiac magnetic resonance strain measurements using feature tracking and conventional tagging, IJC Heart & Vasculature, 18, 46-51

Table 1 Cauchy stresses in remote and MI regions as a function of MI age at 1.15 uniaxial stretch

Infarct age	Remote		MI	
	σ_c (kPa)	σ_l (kPa)	σ_c (kPa)	σ_l (kPa)
Control/normal	1.89±0.71	2.38±0.75	1.90±0.32	5.37±3.41
4h	4.76±1.13	3.08±0.10	5.35±2.44	20.00±5.09
1wk	5.86±0.66	10.93±2.29	17.02±1.16	30.47±4.50
2wk	2.48±0.52	4.65±1.83	33.20±14.08	25.97±10.73
6wk	1.62±0.43	3.02±0.83	11.34±4.63	5.22±2.83

The experimental data are adapted from [227].

Table 2 LV wall stress at rupture site and tensile strength at 1d after MI

Infarct age	LV wall stress (kPa)		Tensile strength (kPa)	
	Mean±SEM	Sample size	Mean±SEM	Sample size
Normal	2.5±0.02	9	2.3±0.03	8
Septum	1.9±0.01	15	1.5±0.02	8
Non-reperfused	2.4±0.04	5	2.4±0.03	12
Reperfused	1.7±0.02	4	1.6±0.01	12

The experimental data are adapted from [251].

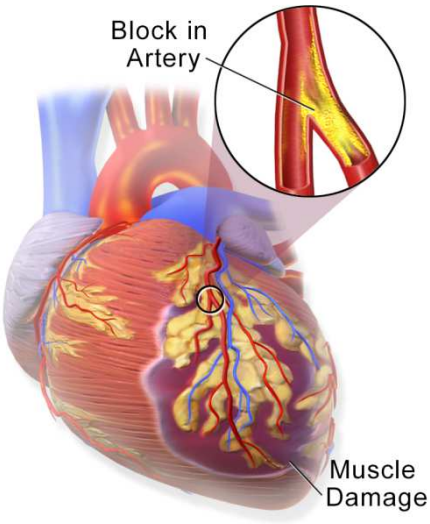

Fig. 1
https://en.wikipedia.org/wiki/Myocardial_infarction#/media/File:Blausen_0463_HeartAttack.png

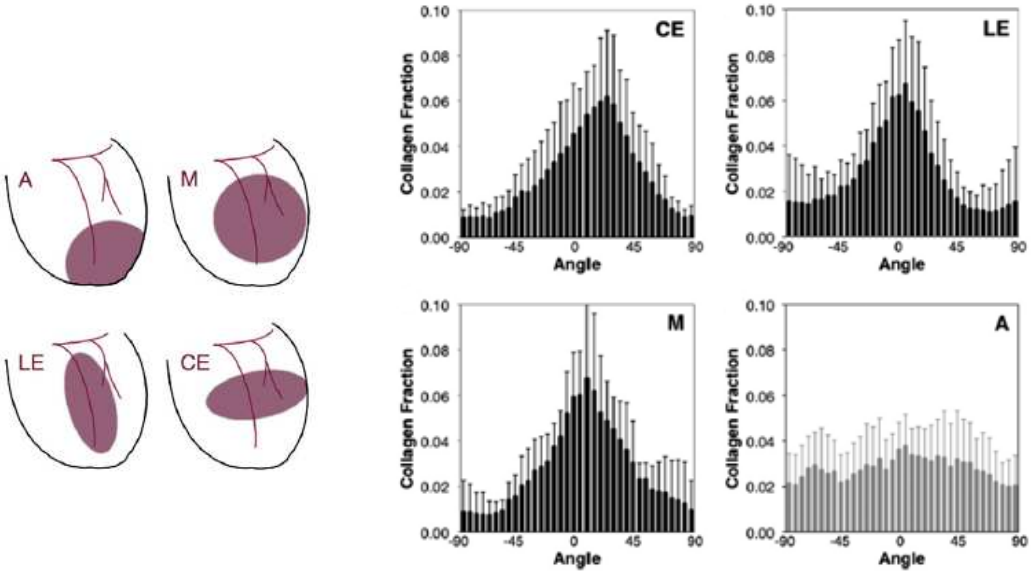

Fig. 2 Collagen orientation histograms at 3wk after myocardial infarction of in 53 Sprague-Dawley rat LVs, the pictures are after [87]

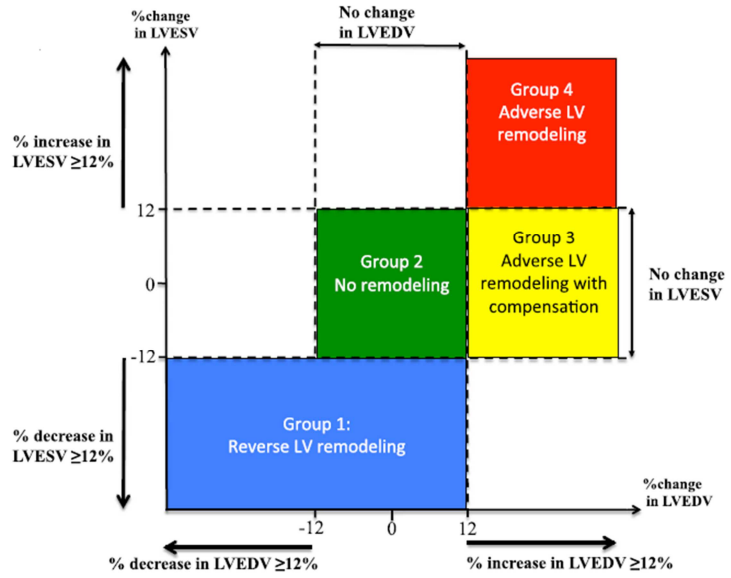

Fig. 3 Four different groups of remodelling based on 12% change in ΔLVEDV and ΔLVESV between 5mth and 2d after acute MI [172]

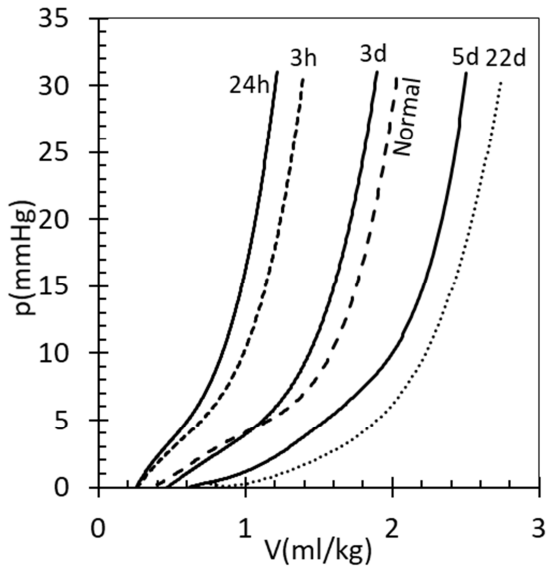

Fig. 4 Mean LV pressure-volume curves at various MI ages in the rat model

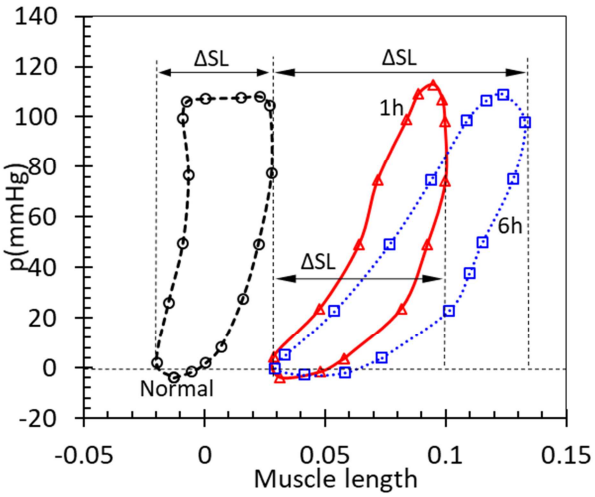

Fig. 5 Pressure-length loops in terms of instant pressure and segment length from single cardiac cycle, ΔSL -phasic segment-length amplitude

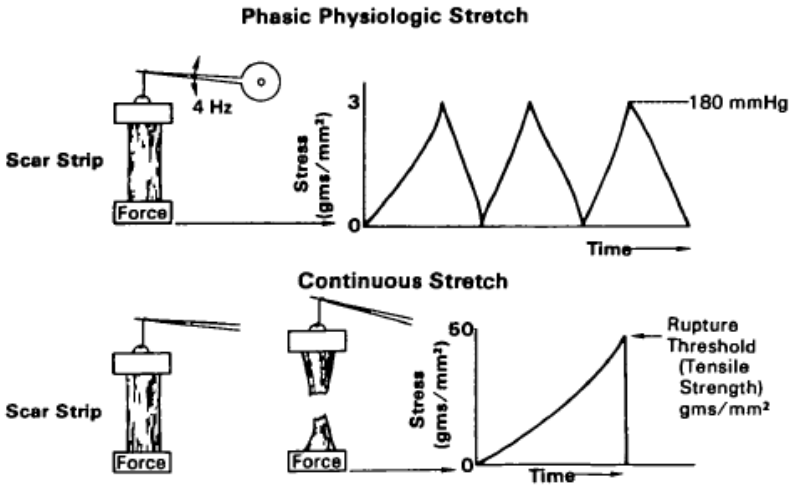

Fig. 6 Sketch of apparatus for uniaxial testing scar tissue elasticity and stretch, the pictures are from [245]

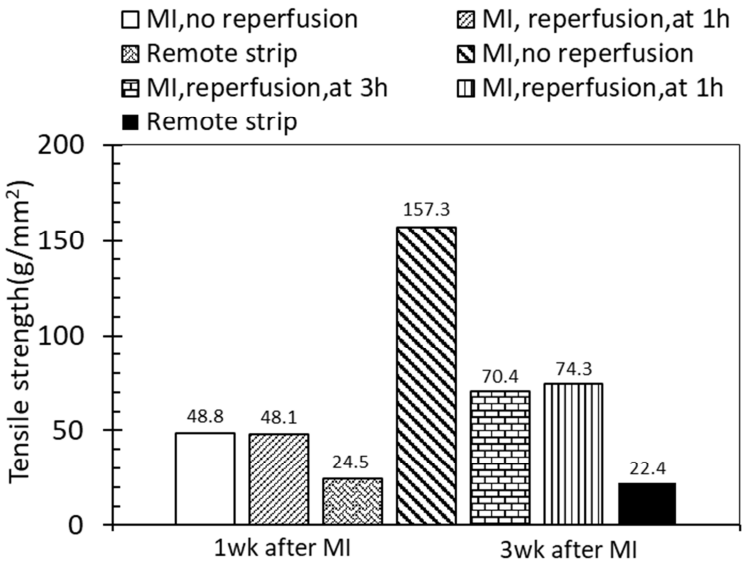

Fig. 7 Effect of reperfusion on tensile strength (rupture threshold) at 1 and 3wk after MI

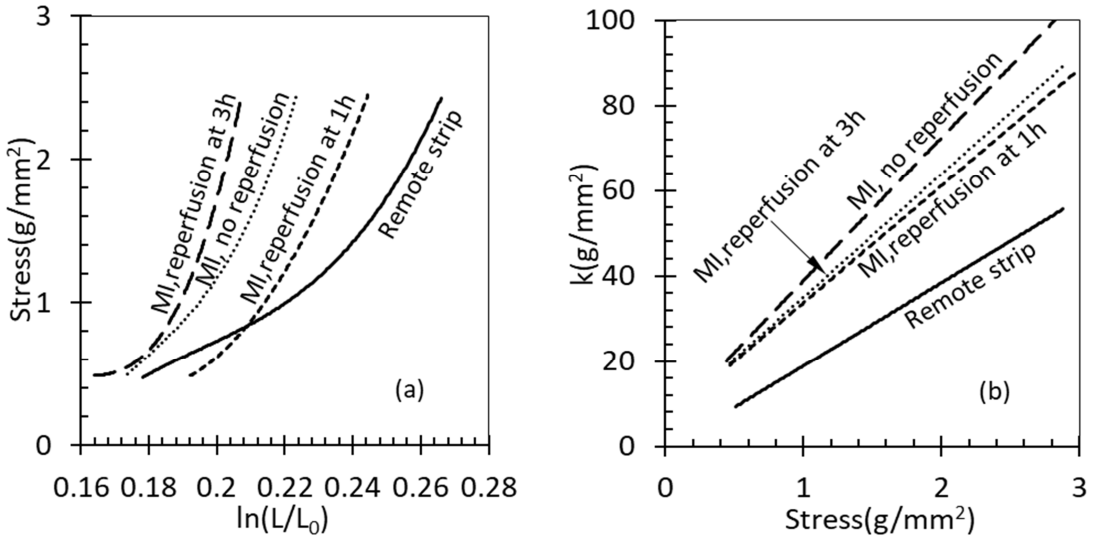

Fig. 8 Effect of reperfusion on stress-strain curve (a) and stiffness (b) at 3wk after MI, Scar and myocardium specimens were stretched and released by phasic physiological stretch at 4Hz

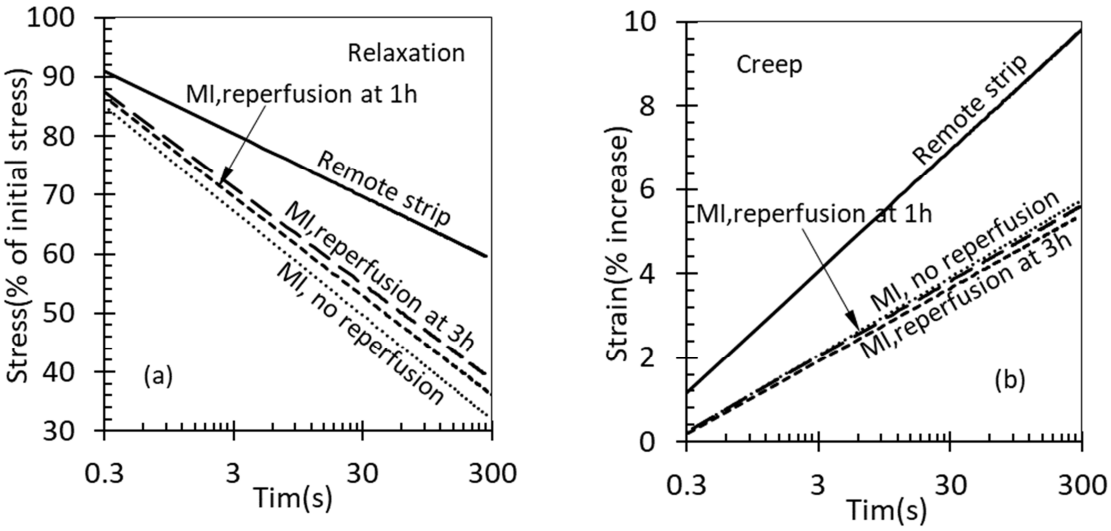

Fig. 9 Effect of reperfusion on viscoelastic properties at 3wk after MI, stress relaxation is expressed by the % decrease in stress from an initial stress level of 3g/mm^2 at a constant length held for 5min, creep is considered the % increase in length in 5min at a constant stress of 3g/mm^2

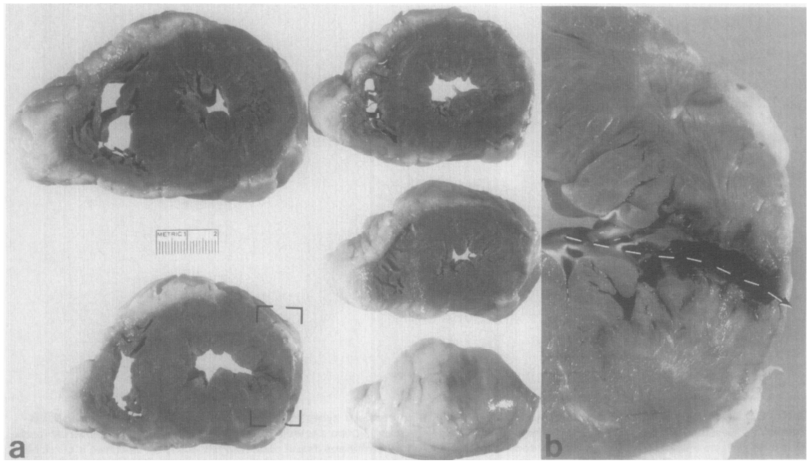

Fig. 10 Transverse images and rupture site of the LV of a 75-year-old with acute MI 4days before death, (a) transverse images, (b) close-up view of the image with brackets to show rupture site(arrow), the pictures are from [247]

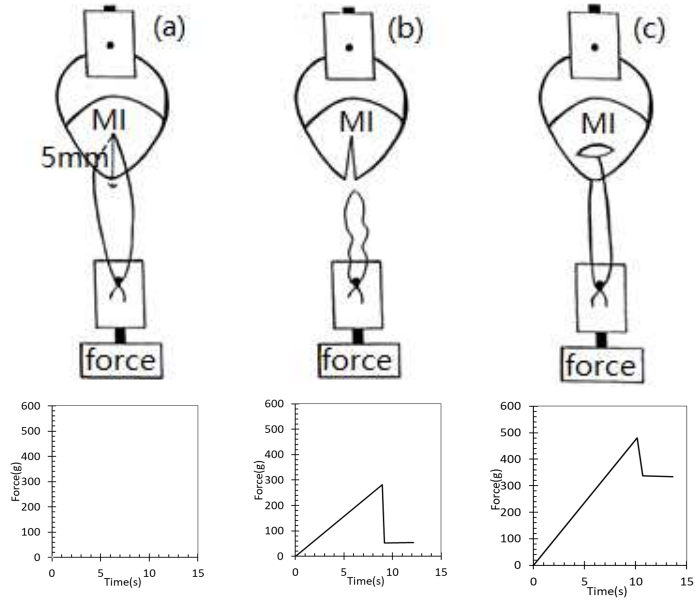

Fig. 11 Method for measuring of tear threshold of infarcted and normal LV myocardium, (a) LV in position, (b) completer tear, (c) partial tear, the pictures are adapted from [251]

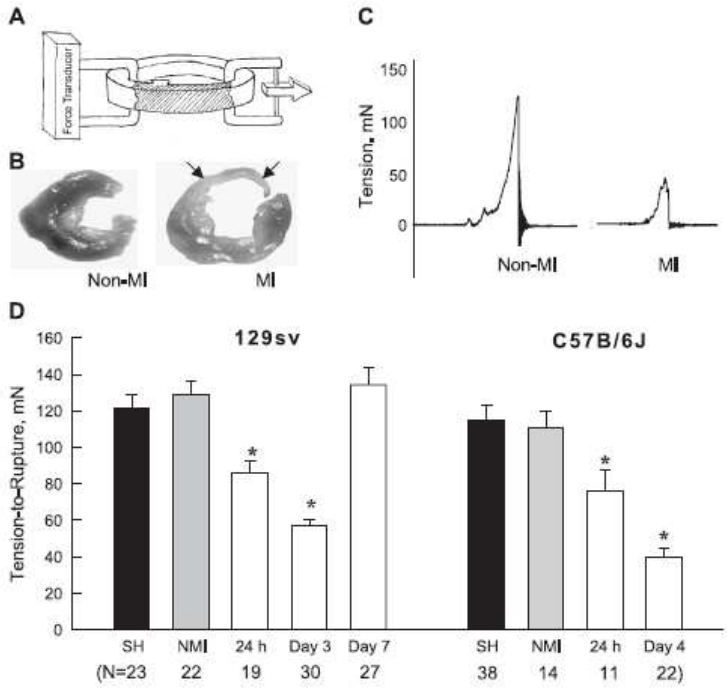

Fig. 12 Measured rupture tension rupture of mice 129sv male mice and C57B/6J mice at various MI ages, the pictures are from [252]